Investigation of Summer Phytoplankton Community in the East China Sea: Analysis of HPLC Pigment and Multiple Excitation Fluorometer Data

(東シナ海における夏季の植物プランクトン群集の研究:

HPLC 色素および多波長励起蛍光光度計データ解析)

XU, Qian

(徐 倩)

A dissertation for the degree of Doctor of Science

Department of Earth and Environmental Sciences,

Graduate School of Environmental Studies, Nagoya University

（名古屋大学大学院環境学研究科地球環境科学専攻学位論文博士（理学））

2021

Abstract

Phytoplankton community play a crucial role in determining the marine food web as well as the structure and function of the marine ecosystem, and respond quickly to environmental changes such as water properties. In the large continental shelf of the East China Sea (ECS), eutrophic low saline Changjiang Water discharging from Changjiang Estuary, diluted by offshore water and formed Changjiang Diluted Water (CDW). On the other hand, Kuroshio Water (KW) flowing from southwest to northeast along the continental shelf break, mixes with surface Changjiang Diluted Water (CDW), and intrudes onto the continental shelf with additional nutrient supplied in subsurface layers. Few inter-annual investigations on horizontal and vertical directions of phytoplankton community were reported in the ECS, although this area is influenced by both fresh and Kuroshio water forming complex mixture condition of the water masses and those water masses changed year by year. In this study, the high performance liquid chromatography (HPLC) method which enable to detect whole structure of phytoplankton communities, was applied in surface observations to explain interannual variations of phytoplankton communities in the ECS. Secondly, a multiple excitation fluorometer, which can provide high-resolution vertical profiles of phytoplankton composition, was applied to understand the response of phytoplankton community in three different water masses of CDW, KW and Tsushima Water (TW).

In Chapter 2, surface distribution of phytoplankton community was investigated in the mid-shelf of the ECS, in July 2009, 2010, 2011 and 2013. HPLC pigments-based analysis tool, CHEMTAX, revealed the dominance of cyanobacteria (including prochlorophytes) for all four years in the eastern ECS which was perennially under influence of the oligotrophic KW. On the mid-shelf ECS, the composition of phytoplankton communities varied from year to year. Diatoms dominated in 2009 and 2013 when dissolved inorganic phosphate (DIP) concentrations were higher than 2010 and 2011. During 2010 and 2011 characterized as high-nitrate-years, a mixed population of cyanobacteria, chlorophytes and other groups was observed. Cluster analysis based on the phytoplankton community composition, together with Principal Component Analysis of shipboard hydrographic and nutrient data for all four years helped to confirm that summer phytoplankton community structure on the mid-shelf ECS was regulated by the nutrient (N:P) ratio. Nutrient concentration in Changjiang river discharge and the extent of water mixing with upwelled subsurface waters from the coastal region were supposed to have influenced the nutrient ratios and the phytoplankton composition within CDW.

In Chapter 3, vertical distributions of phytoplankton composition in the ECS and Tsushima Strait were observed from an in-situ multiple excitation fluorometer which was rarely used in oceanographic study. The data was calibrated with HPLC data to make high-resolution vertical data in every meter of the water column. KW region were featured with deep chlorophyll maxima (SCM) below 40 m with chlorophyll a less than 1 mg m^{-3} until the SCM. High fraction of cyanobacteria (>40%) extended deeply to 30 m at depth, brown algae became dominated (>50%) in deep layer below 40 m including SCM. In TW, CHL were higher than KW but lower than CDW, brown algae were predominated in most of the water column (>60%) and in SCM (30-55 m), except the low nutrient surface layers where cyanobacteria was dominated. In the CDW, where SCM were observed at relatively shallow layers around 15-30 m, brown algae (diatoms and dinoflagellates) were generally presented in less than 60% even the highest CHL was observed among the three regions, and cyanobacteria (>40%) and green algae plus cryptophytes (>40%) were observed at above and below SCM, respectively. The usefulness of multiple excitation fluorometer was shown to understand the detailed vertical distribution of phytoplankton community in the highly variable region like ECS.

This study showed the importance of interannual variation of the wind driven coastal upwelling which may elevate DIP concentration in CDW to support diatoms and dinoflagellates growth, in addition to the previous conclusion on DIP limitation on phytoplankton growth in CDW. Furthermore, it is clearly indicated that the newly calibrated in-situ multiple excitation fluorometer is useful to obtain the high-resolution vertical profiles of phytoplankton groups in highly variable coastal waters.

Contents

List of Tables

List of Figures

Fig. 2.5. (a) CHL concentration versus Excess Nitrate (ExcN) in high-DIP-years (+) and high-NOx-years (○). (b) CHL concentration versus DIP in the surface East China Sea for all four years. $p < 0.05$ indicates that CHL was significantly different between high-DIP-year (+) and high-NOx-year (○). Dashed grey lines in (a) indicated N:P = 16, in (b) indicated the detection limit of DIP (0.01 μM).

Fig. 2.6. Abundance of phytoplankton communities versus Excess Nitrate (ExcN) in the surface ECS during high-DIP-year (+) and high-NOx-year (○). $p < 0.05$ indicates that phytoplankton concentration was significant different between high-DIP-year (+) and high-NOx-year (○).

Fig. 2.7. Dendrogram of cluster analysis based on phytoplankton composition.

Fig. 2.8. Averaged values of surface phytoplankton composition and DIP (a) and temperature and salinity (b) in each cluster in the mid-shelf of the ECS. Black line indicates averaged DIP concentration.

Fig. 2.9. Relative abundances of surface phytoplankton communities in T-S plots in the ECS for the four years. Clusters are indicated by different colors. Dashed lines divide water masses according to salinity as CDW (< 30), SW (30-32.9) and KSW (> 32.9).

Fig. 2.10. Relative abundances of surface phytoplankton communities in DIP-NO_x plots in the East China Sea for four years. Clusters are indicated by different colors. Dashed lines indicated detection limit of nutrients (DIP: 0.01 μM, NO_x: 0.05 μM). Solid line

indicates N:P =16.

Fig. 2.11. Principal Component Analysis of the phytoplankton composition and environmental factors in the ECS. Colors of vectors: black indicate phytoplankton, blue indicates physical parameters, and red indicates chemical parameters.

Fig. 2.12. Relationship between surface DIP and salinity for all stations in this study; (+) 2009/2013 and (○) 2010/2011. The dotted line is obtained from Zhang et al. (2007).

Fig. 2.13. Schematic of interannual variation of summer phytoplankton community distribution in the ECS; (a) Mixed populations of cyanobacteria, chlorophytes, diatoms and dinoflagellates exist in DIP limited water as a result of high N:P ratio of the CDW (cf. 2011/2012), (b) Diatom dominates in no-DIP-limited water resulted by mixing of CDW with low N:P upwelled water near the coast (cf. 2009/2013). Dino.: dinoflagellates, Chhloro.: chlorophytes, Cyano.: cyanobacteria, Prym.: prymnesiophytes, Prochloro.: prochlorophytes.

Fig. 2.S1. Weekly Sea Surface Temperature anomaly (SST A) (https://mur.jpl.nasa.gov/) calculated from weekly SST, and overlaid with weekly wind intensity (arrows) (http://www.remss.com/) in the third week of July 2009, 2010, 2011 and 2013.

Fig. 3.1. Sampling locations for the four cruises in the East China Sea (ECS) and Tsushima Strait in late July of 2011 - 2014. Three transects (dashed line) and three

representative stations (inverted triangle) in Changjiang Diluted Water (St-CDW), Tsushima Water (St-TW) and Kuroshio Water (St-KW) were selected to compare vertical profiles of water properties and phytoplankton distributions.

Fig. 3.2. Monthly composites of SST (°C) and CHL (mg m^{-3}) in the ESC and TS during 2011-2014 in July.

Fig. 3.3. (a) Temperature-salinity (*T-S*) plot of the upper 100 m depth delineating water masses. CDW (Y) were defined as T > 23°C, S < 30, KW (+) were defined as T > 23 °C, S >= 32.9, KSSW (Δ) were defined as T <19 °C, and the rest data were defined as Mixed Water (O). (b) Depth of the samples of the *T-S* plot.

Fig. 3.4. Distribution of each water mass that defined in Fig. 3.3. in the study areas.

Fig. 3.5. Vertical distributions of temperature (°C) (a-c), salinity (d-f) in the tree selected transects .Black dots are sampling data.

Fig. 3.6. Vertical distributions of NOx (a-c), SiO2 (d-f), DIP (g-i) (μM) and N:P (j-l) in the tree selected transects. Black dots are sampling data.

Fig. 3.7. CHL concentrations (mg m-3) (a-c)and the relative abundance of phytoplankton groups (a-o) estimated by Multi-Exciter in the three selected transects. Black dots are sampling data.

Fig. 3.8. Vertical profiles of environmental factors (a-h) and Multi-Exciter-derived phytoplankton groups during the four courses i-j, 2011: red, 2012: green, 2013: blue,

2014: yellow) and the representative stations (m-p) for each water.

Fig. 3.9. Comparison between HPLC-CHEMTAX (left) and the Multi-Exciter (right) derived vertical profiles of phytoplankton compositions. The colored dots were samples measured by the HPLC method; these samples overlayed on the profiles presented by the fluorometer and marked with black circles.

Abbreviation

Allo	Alloxanthin (mg m^{-3})
A_SCM	Above Subsurface Chlorophyll *a* Maximum
B_SCM	Below Subsurface Chlorophyll *a* Maximum
CDW	Changjiang Diluted Water
CHL	Chlorophyll *a*
DIN	Dissolved inorganic nitrogen or NOx (NO_3^-+NO_2^-)
DIP	Dissolved inorganic phosphorus or PO_4^{3-}
ECS	East China Sea
ExcN	Excess Nitrate
HPLC	High Performance Liquid Chromatography
KIW	Kuroshio Intermediate Water
KSSW	Kuroshio Subsurface Water
KSW	Kuroshio Surface Water
KW	Kuroshio Water
NOx:DIP or N:P	DIP versus NOx
PCA	Principal Component Analysis
SCM	Subsurface Chlorophyll a Maximum
SST	Sea Surface Temperature
SW	Shelf Water
TS	Tsushima Strait
T-S plot	Temperature-Salinity Plot
TW	Tsushima Water
TWC	Taiwan Warm Current
Fucox	Fucoxanthin
Perid	Peridinin
19butfu	19’-butanoyloxyfucoxanthin
19hexfu	19’-hexanoyloxyfucoxanthin
zeax	Zeaxanthin
neox	Neoxanthin
Chlb	Chlorophyll *b*
Violax	Violaxanthin
Prasinox	Prasinoxanthin
DV-Chla	Divinyl-chlorophyll *a*

Symbols

$c0$	regression coefficients between phytoplankton group fractions and PC scores (Si)
ci	regression coefficients between phytoplankton group fractions and PC scores (Si)
f	CHL fractions of brown algae, cyanobacteria, or green algae
$F(\lambda)$	spectral features from phytoplankton fluorescence excitation spectra
Si	the i-th PC score

Chapter 1 General Introduction

1.1 Complex characteristics of water masses in the ECS

The East China Sea (ECS) surrounded by China, Japan and Korea is one of the largest continental shelves that supporting rich fishery resources. It stands as an important passage for material transports from the Yellow Sea and East China Sea to the Tsushima Strait (TS), onwards into the Sea of Japan (Chen and Wang 1999; Isobe 1999). The ECS is featured with complex water current system associated with three distinct water masses, including the Changjiang River Diluted Water (CDW), Taiwan Warm Current (TWC) and Kuroshio Current. The CDW is a mixed water mass formed by low salinity high nutrient Changjiang River discharge and high salinity low nutrient offshore water. Strongly influenced by the anthropogenic activities, the input of dissolved inorganic nitrogen (DIN) from Changjiang River is much higher than dissolved inorganic phosphorus (DIP) (N:P ratio > 100) (Wang and Wang 2007; Chen 2008, Xu et al., 2018). DIP is fast consumed by phytoplankton as frequently phytoplankton bloom happened at Changjiang Estuary, resulting in the increased DIP-limitation from inshore to offshore areas (Liu et al., 2016). . On the other hand, Taiwan Warm Current originated from Kuroshio Current with warm saline and oligotrophic water at surface, flowing along Chinese coast from south to north. Nutrient is also depleted in the surface layer of the Kuroshio Current; however, the nutrient-rich subsurface water intrudes into the shelf of ECS and mixed with TWC. This process produces upwelling that supports longer phytoplankton blooms around Changjiang Estuary, and changes the nutrient stoichiometry of CDW (Chen et al. 2004; Yang et al. 2013; Tseng et al. 2014).

1.2 Measurement of phytoplankton communities in the ECS

Phytoplankton communities determine the structure and function of marine ecosystem, changes on the community structures in response to physical and chemical environments directly on higher trophic levels and on biogeochemical cycling in the ocean (Simpson and Sharples, 2012; Goes et al. 2014). For the ECS, large gradients of water properties between inshore and offshore formed high variability of phytoplankton community structures during summer. As a result, satellite observations showed large seasonal and spatial variability of chlorophyll a concentrations (CHL) associated with the movement of the CDW, with high phytoplankton productivity (CHL > 60 mg m^{-3}) observed in the Changjiang estuary and adjacent areas, but lower CHL (< 1 mg m^{-3}) in the outer shelf in summer (Yamaguchi et al. 2012; 2013). High performance liquid chromatography (HPLC)-based studies albeit limited in spatial extent have shown that cyanobacteria were abundant in the oligotrophic Kuroshio waters, while diatoms and dinoflagellates dominate in the Changjiang Estuary and adjacent areas (Furuya et al.

2003; Zhu et al. 2009; Liu et al. 2016). However, lack of interannual *in-situ* biogeochemical datasets have hampered a better understanding on how interannual variations of mixing of different water masses in the ECS impact seawater nutrient composition, one of the important drivers of phytoplankton community structure. Furthermore, the cost of water sampling and lab analysis have greatly limited the sampled data measurements and data resolution to explore intensive phytoplankton variations in vertical and in large-scale observations.

1.3 Research objectives and thesis structure

Under the mixing effect among different water masses, we hypothesize that phytoplankton communities in the mid-shelf ECS would be more variable. However, previous studies mostly stressed on the Changjiang Estuary, which hampered the understanding about the potential influencing factors in relationship between physical and chemical water properties and phytoplankton communities. Thus, the objective of this study is to investigate how phytoplankton community's changes in response to water properties by inter-annual observations of phytoplankton compositions in surface layer of the mid-shelf ECS. In addition to surface observations, the multiple excitation fluorometer data with *in-situ* calibration provided high-resolution vertical profiles which were used to describe vertical distributions of phytoplankton in the transections of different water masses.

This thesis includes 5 chapters. In Chapter 1, general introduction of research background and objectives are included. In Chapter 2, HPLC pigment-based analysis are used to derive phytoplankton compositions in July, 2009, 2010, 2011 and 2013, the time period when the river discharge is at a maximum. In Chapter 3, an *in-situ* multiple excitation fluorometer is applied and calculated to interpret vertical profiles of phytoplankton composition in the three distinguished water masses: CDW, KW and TW. Chapter 4 gives a general discussion about the findings of this thesis. Chapter 5 concludes finding from previous chapters and provides suggestions for further researchers.

Chapter 2 Inter-annual changes in summer phytoplankton community composition in relation with water mass variability in the East China Sea

2.1 Introduction

Phytoplankton communities play a crucial role in determining the marine food web as well as the structure and function of the marine ecosystem (Lalli and Parsons 1997). Large phytoplankton, such as diatoms and dinoflagellates, are important for sustaining the high productivity and fertile fishing grounds of coastal and upwelling areas. Small phytoplankton like cyanobacteria, which profit from their high nutrient utilization efficiency, are more abundant in the open ocean and are essential in supporting the microbial loop of oligotrophic oceans (Finkel 2007).

The East China Sea (ECS), which is surrounded by China, Korea and Japan, is one of the largest continental shelves and a fertile fishing ground. It features a complex current system that includes influences of euryhaline coastal and saline oceanic water masses (Gong et al. 1996; Chen 2008). A major oceanic current into the ECS is the Kuroshio current. Kuroshio surface water which is nutrient depleted (NO_3^-+NO_2^- (NOx) < 0.2 μM, PO_4^{3-} (DIP) < 0.05 μM, N:P < 16) (Chen 2008), intrudes into the ECS via two major branches, one from the northeast of Taiwan and the other from the southwest of Kyushu (Fig. 2.1) (Guo and Miyazawa 2006). To the east, the Changjiang River (also known as Yangtze River), the third largest river in the world, discharges large amounts of freshwater containing extremely high concentrations of anthropogenically-derived nutrients from inland China into the ECS. During summer, when river-runoff is at its peak, NOx concentration can exceed 50 μM and DIP concentration > 1 μM (Zhang et al., 2007).

Satellite observations showed large seasonal and spatial variations of chlorophyll a concentrations (CHL) associated with the movement of the CDW, with high phytoplankton productivity observed in the Changjiang estuary and adjacent areas close to the coast, but lower CHL concentrations in the outer shelf in summer (Yamaguchi et al. 2012; 2013). In general, phytoplankton community composition in between the shelf waters and the open ocean can vary widely in response to large gradients in physical and chemical properties across the continental shelf (Simpson and Sharples 2012; Goes et al. 2014).

Microscopy has been employed to compile information on large phytoplankton (> 20 μm) such as diatoms and dinoflagellates (Guo et al. 2014; Li et al. 2009; Jiang et al. 2015), while picoplankton (< 2 μm) have been largely identified and enumerated using flow cytometry (Jiao et al. 2005; Lee et al. 2014; Pan et al. 2007). Chemotaxonomy, the identification of phytoplankton from several phytoplankton groups based on ‘diagnostic pigments' which are specific to individual phytoplankton taxa or groups (Jeffrey et al. 1997) provides a more convenient method to estimate the entire range of the phytoplankton community. High performance liquid chromatography (HPLC)-based studies albeit limited in spatial extent have shown that cyanobacteria were abundant in the oligotrophic Kuroshio waters, while diatoms and dinoflagellates dominate in the Changjiang Estuary and adjacent areas (Furuya et al. 2003; Zhu et al. 2009; Liu et al. 2016).

The mid-shelf ECS is an important passage for materials transportation from the Yellow Sea and South China Sea to the Tsushima Strait and onwards into the Sea of Japan (Chen and Wang 1999; Isobe 1999), but it has been poorly understood and only sparsely studied. This region is covered by Changjiang River Diluted Water (CDW) which is formed by mixing with offshore waters influenced by Kuroshio Surface Water (KSW) (Wang et al. 2014; Zhu et al. 2017). CDW is believed to be DIP-limited (N:P > 100) because DIP is fast consumed by phytoplankton blooms out of Changjiang Estuary (Wang and Wang 2007; Chen 2008). Along the coastal area of China, coastal upwelling of Taiwan Warm Current and inshore intrusion of Kuroshio Intermediate Water (KIW) are known to support higher and longer phytoplankton blooms around Changjiang Estuary and responsible for changing the nutrient stoichiometry of CDW (Chen et al. 2004; Yang et al. 2013; Tseng et al. 2014). However, lack of interannual *in-situ* biogeochemical datasets have hampered a better understanding on how interannual variations mixing of different water masses in the ECS impact seawater nutrient composition, one of the important drivers of phytoplankton community structure.

In this study, we hypothesize that phytoplankton composition in the mid-shelf ECS can be impacted by variations in the mixing of different water masses, in particular the flow and the extent of mixing of the CDW and the Kuroshio because of differences in their nutrient content. Since this investigation is based on summer-time data, a time period when the river discharge is at a maximum, and for four years, i.e. 2009, 2010, 2011 and 2013, it allows us to provide a more mechanistic explanation of how inter-annual variability in water mass mixing impacts phytoplankton communities of the ECS ecosystem.

2.2 Materials and Methods

2.2.1 Study area and sampling regime

In-situ sampling was undertaken in the ECS on shipboard expeditions aboard the T/V *Nagasaki Maru* in late July of 2009, 2010, 2011 and 2013 as shown in Fig. 2.1. All stations were located in the ECS from 124.6 to 128.8 ^{o}E and from 31.4 to 33.0 ^{o}N. At each station, a CTD was used to profile temperature (T) and salinity (S) in the upper 80m. Water samples for *chlorophyll a* (CHL) as well as other phytoplankton pigments and nutrients (including $NO_x = NO_3^- + NO_2^-$, DIP: PO_4^{3-}) were collected at the sea surface using an acid washed bucket. Nutrient samples were immediately frozen in polyethylene tubes after sampling and transferred under frozen conditions to the shore laboratory for analysis using an auto-analyzer (TRACCS 2000, BL Tech). NOx and DIP concentration were determined according to absorption spectrometry (Armstrong et al. 1967; Murphy and Riley 1961; Koroleff 1983).

Water samples for HPLC pigment analysis (1-2 L) were filtered through 25 mm Whatman GF/F glass fiber filters under vacuum pressure (< 0.01 MPa) in dim light, and then immediately frozen in liquid nitrogen until the samples were analyzed in the shore laboratory. Phytoplankton pigments were separated and measured in methanol extracts using the reverse-phase HPLC method of Heukelem and Thomas (2001), and a Zorbax Eclipse XDB-C8 column (150 mm × 4.6 mm, 3.5 μm; Agilent Technologies).

Excess nitrate (ExcN) in seawater samples was calculated to evaluate DIP limitation using the formula $ExcN = NOx - R \times DIP$ (Wong et al. 1998), where R is the Redfield ratio of 16 (NOx:DIP or N:P) (Redfield 1963). Therefore, ExcN values < 0 (N:P < 16) indicate DIP-enrichment, while ExcN > 0 μM (N:P > 16) indicate DIP-limitation (Wong et al. 1998).

2.2.2 CHEMTAX derived phytoplankton groups

The contribution of various phytoplankton groups to the overall CHL pool was estimated from the array of HPLC separated pigments and calculated using CHEMTAX (Mackey et al. 1996). Matrices of pigment data and initial pigment ratios (i.e. pigment to CHL ratio for each phytoplankton group) (Table 1) were used as inputs into the CHEMTAX program (Mackey et al. 1996; Suzuki et al. 2002). 12 marker pigments (chlorophyll *a*, fucoxanthin, peridinin, 19'-butanoyloxyfucoxanthin, 19'-hexanoyloxyfucoxanthin, zeaxanthin, neoxanthin, chlorophyll *b*, violaxanthin, alloxanthin, prasinoxanthin, divinyl-chlorophyll *a*) were selected and classified into 9 phytoplankton groups (prasinophytes, dinoflagellates, cryptophytes, prymnesiophytes, chrysophytes, chlorophytes, cyanobacteria, prochlorophytes, diatoms) based on earlier research that also employed CHEMTAX to study phytoplankton composition in the ECS (Furuya et al. 2003; Zhu et al. 2009) (Table 1). Note that prochlorophytes were excluded from cyanobacteria in this study. To derive the most accurate phytoplankton groups from the marker pigments, CHEMTAX was run on surface datasets of 2009, 2010, 2011 and 2013 separately. For each dataset, CHEMTAX program was run 10 times by using the output ratio matrix of the last run as the next ratio matrix input (Latasa 2007). Optimized phytoplankton compositions were selected from the most stable final ratios among the 10 outputs (Table 1).

2.2.3 Statistical analyses

Principal Component Analysis (PCA) and Cluster Analysis were performed using

JMP Pro 11 software. CHL contribution of dinoflagellates, chlorophytes, prymnesiophytes, cyanobacteria, prochlorophytes and diatoms derived from CHEMTAX at all 76 stations for the four years were used for the statistical analyses. PCA was used to examine the correlations between the selected phytoplankton groups and environmental factors (Goes et al. 2014). The Ward minimum variance method (Ward 1963) was used to group the stations into clusters based on similarities in phytoplankton compositions and water mass properties including salinity and ExcN (Dorado et al. 2015; Fujiwara et al. 2014). The analysis resulted in four major clusters which shared specific environmental features and phytoplankton functional groups. To compare average values from 2009/2013 and 2010/2011, a non-parametric Mann-Whitney U test was performed using the software Origin pro 8.0. Differences between datasets over four years were considered significant when $p < 0.05$ (Salkind 2006).

2.3 Results

2.3.1 Hydrography

A temperature versus salinity (*T*-*S*) plot for samples from the upper 80 m depicts four major water masses in the ECS (Fig. 2.2 a). The presence of the Changjiang River plume in near surface layers was obvious from its < 28 salinity and > 23 ^{o}C temperature signatures. Based on previous studies, the CDW boundary was defined as salinity < 30 (Zhang et al. 2007; Zhou et al. 2008). A higher salinity (> 34), warmer water mass in upper layers was associated with deeper high-salinity Kuroshio water (KW) (Gong et al., 1996; Umezawa et al. 2014; Zhou et al. 2008). KSW was defined with salinity > 32.9, while shelf water (SW) was defined with salinity ranging from 30.0-32.9. SW was located in the central part (125-128 ^{o}E) of our study area. In the KSW, vertical density from the surface to the deeper layers showed small gradients ranging from 20.7 to 24.7, whereas sharper density gradients ranging from 14.2 to 20.2 were seen in the CDW. Stations in 2010/2011 showed strong water column stratification and strong pycnoclines, whereas stations in 2009/2013, were relatively homogeneous with density from 18.0 to 20.6 in the shallow layers.

At KSW stations, NOx and DIP was depleted above 45 m, but increased slightly at deeper depth (Fig. 2.2 b, c). Distinct variations were observed in NOx and DIP concentrations in the surface of the CDW stations between 2010/2011 and 2009/2013. In 2010/2011, at depths < 20 m, NOx was high (> 5 μM), whereas DIP was depleted. Conversely, relatively higher DIP (> 0.2 μM) was observed in 2009/2013 in the surface layers. Bottom DIP concentrations were much higher in nearshore stations than at the KSW stations where DIP measured around 1-2 μM and NOx was 8-16 μM. This resulted in low N:P < 10 in the bottom layers. It is observed that even at the stations with high surface NOx or DIP, the high values were not continuous from the bottom to the surface, and there were layers of relatively low concentration around 10-30 m deep. The surface high NOx or DIP waters were characterized by relatively low salinity, indicating that the high nutrients were associated with CDW and not caused by local mixing or upwelling.

Surface temperatures ranged from 24.8 to 29.5^{o}C, with high and low values observed in the east and west, respectively (Fig. 3 a - d). Salinity patterns corresponded with temperature distributions showing low (< 30) and high (> 32.9) salinity in the west and east, respectively. Warm and high salinity waters that characterized the KSW were observed east of our study area around 128.7 ^{o}E during all four years (Fig. 2.3e - h). The extent of the CDW varied, it spread eastward to 126 ^{o}E in 2009, 2011, 2013 (Fig. 2.3 e, g, h), while it covered almost the entire study area in 2010 except for the easternmost part which was dominated by the KSW.

Surface oligotrophic conditions (NOx < 0.11 μM, DIP < 0.07 μM) prevailed during all four years in KSW (Fig. 2.3 i - p). Toward the west, in the SW, both NOx and DIP concentrations increased gradually, while noticeable interannual variations were seen in the CDW where salinity < 30. Extremely high NOx (> 10 μM, maximum of 26.1 μM) but low DIP (< 0.05 μM) and ExcN > 0 were observed in 2010/2011 (Fig. 2.3 j, k), in contrast to the relatively lower NOx (< 2 μM), higher DIP (> 0.1 μM) and ExcN < 0 waters in 2009/2013 (Fig. 2.3 i, l, m, p). Differences in nutrient concentrations between 2009/2013 and 2010/2011 in the CDW and the SW were statistically significant ($p < 0.01$). Average values of NOx, DIP and ExcN were 0.68 μM, 0.19 μM and -2.39 μM, respectively, for 2009/2013, and 4.55 μM, 0.06 μM and 3.63 μM for 2010/2011 (Fig. 2.3 i - t). Hereafter, we define 2009/2013 as high-DIP-years and 2010/2011 as high-NOx-years.

2.3.2 Surface phytoplankton distribution

Overall, surface CHL was higher in the CDW (0.25-3.99 mg m^{-3}) (Fig. 2.4 a), and lower in the SW (0.14-0.88 mg m^{-3}) (Fig. 2.4 b). Lowest values were observed in KSW where CHL rarely exceeded 0.17 mg m^{-3} (Fig. 2.4 c). CHEMTAX analysis revealed that the low CHL at those stations was derived from a mixture of cyanobacteria and prochlorophytes which accounted for > 61% of the total CHL in KSW over the four years (Fig. 2.4 c). Prochlorophytes comprised more than 30% of the phytoplankton community in 2009/2010 and 2013, and 19% in 2011 (Fig. 2.4 c). Outside of the KSW region, diatoms were more widely distributed and in higher numbers in 2009/2013 (Fig. 2.4 a). Compared to diatoms, dinoflagellate population was a minor component of phytoplankton communities, but it was relatively higher in 2009/2013 compared with 2011/2012 (Fig. 2.4 a). Prymnesiophytes were generally lower as compared to diatoms but were higher in the mixed waters of the SW in 2011/2013 (Fig. 2.4 b). Inter-annual differences in the average composition of diatoms, dinoflagellates and cyanobacteria were statistically significant ($p < 0.05$), excluding those in the KSW. Average values for samples in the CDW and the SW revealed that diatoms and dinoflagellates contributed > 57% of CHL in 2009/2013, while other groups including cyanobacteria, chlorophytes and prymnesiophytes accounted for 38, 16 and 17% respectively. Conversely diatoms comprised only 13% of the population in 2010/2011 (Fig. 2.4 a, b).

2.3.4 Relationship between phytoplankton biomass and nutrient concentrations

CHL varied over the four years and was significantly higher during high-DIP-years (2009/2013), but lower during high-NOx-years (2010/2011) (Fig. 2.5 a). A strong negative correlation was observed between CHL and ExcN when ExcN < 0 μM (r^2 = 0.48, n = 39) while a positive correlation was obtained when ExcN > 0 μM (r^2 = 0.37, n = 37) (Fig. 2.5a). Inter-annual variability in CHL appeared to be regulated largely by DIP availability as seen by the high correlation between CHL and DIP (r^2 = 0.46) for data from all four years (Fig. 2.5 b).

Diatoms and dinoflagellates concentrations increased significantly with decreasing ExcN (r^2 = 0.45 and 0.43) and accounted for a large fraction of the high CHL seen during the high-DIP-years (Fig. 2.6 a, b). On the other hand, cyanobacteria and prochlorophytes concentrations were higher when ExcN was 0, but low when ExcN > 0 (Fig. 2.6 c, d). Chlorophytes concentrations were generally higher when ExcN > 0 μM

(r^2 = 0.55) and conversely much lower when ExcN <= 0 μM. No clear relationship could be discerned between prymnesiophytes and ExcN (Fig. 2.6 e).

2.4.5 Statistical analysis

Cluster analysis based on the composition of phytoplankton aided in partitioning all stations sampled during four years into four clusters (Fig. 2.7). Stations in Cluster 1 comprised a mixed population of diatoms (11%), dinoflagellates (12%), cyanobacteria (44%) and chlorophytes (17%). Diatoms and dinoflagellates dominated stations in Cluster 2 accounting for about 66% of the total phytoplankton. Cyanobacteria were the dominant (51%) phytoplankton in stations of Cluster 4 while prochlorophytes made 28% of the population in this cluster. This Cluster was also characterized by stations with the lowest DIP, and highest temperature and salinity (Fig. 2.8 b). Stations in Cluster 3 were composed of cyanobacteria and prymnesiophytes (61%) (Fig 8 a).

Six dominant phytoplankton groups, diatoms, dinoflagellates, cyanobacteria, prochlorophytes, prymnesiophytes and chlorophytes, within each cluster were selected to examine their relationship with surface water properties and nutrient concentrations. Diatoms (> 50%) predominated in waters with salinity ranging from 28.5 to 31.6 and temperatures between 24.9 and 27.7 ^{o}C (Fig. 2.9 a), whereas cyanobacteria (> 50%) populations predominated both low salinity CDW (salinity < 27.5) as well as higher salinity waters (salinity > 31.6) (Fig. 2.9 c). In waters which harbored high proportions of prymnesiophytes, salinities were in excess of 30 and temperatures were higher than 26 ^{o}C (Fig. 2.9 e). Chlorophytes and dinoflagellates accounted for more than 30% of CHL in low salinity waters (Fig. 2.9 b, f), while in high salinity waters prochlorophytes contributed about 30% of CHL (Fig. 2.9 d).

The relationship between different phytoplankton groups and nutrient concentrations (DIP versus NOx) are presented in Fig. 2.10. Generally, diatoms contributed a large fraction of the CHL (~ 80%) in waters with N:P ratios < 16 (or ExcN < 0 μM), followed by dinoflagellates (Fig. 2.10 a, b). High proportions of cyanobacteria especially in Cluster 3 were observed in waters with N:P ratios close to 16; as well as in low nutrient waters where NOx < 0.4 μM and DIP < 0.2 μM (Fig. 2.10 c). Prymnesiophytes, prochlorophytes and chlorophytes were higher in the low DIP waters (Fig. 2.10 d, e, f).

Principle Component Analysis (PCA) using data from all four years was utilized to investigate the influence of environmental factors on the distribution of major phytoplankton groups in the ECS. The first two PCs explained more than 51% of the variations (Fig. 2.11). Salinity showed a strong negative correlation with PC1 while ExcN and NOx, showed strong negative correlations with PC2. It was clear that chlorophytes increased in lower salinity and higher ExcN CDW in 2010/2011. Diatoms and dinoflagellates showed a preference for waters of lower temperatures and high DIP. Cyanobacteria and prochlorophytes were associated with waters of higher temperatures and lower DIP concentrations which are characteristics of the KSW (Fig. 2.11).

2.4 Discussion

2.4.1 Phytoplankton biomass and community composition

Inter-annual variations in CHL were large in the west of the study area and decreased eastward in accordance with variations in temperature, salinity and nutrients brought about by mixing of the KSW, CDW and SW (Fig. 2.3). This distribution is consistent with previous studies (Yamaguchi et al. 2012; 2013) which also showed that CHL concentrations were higher in coastal waters and lower offshore. Interestingly, the high CHL (> 1 mg m^{-3}) during the high-DIP-years of 2009/2013 was largely derived from diatoms and dinoflagellates, while during high-NOx-years of 2010/2011 it was derived from a mixed populations of cyanobacteria, chlorophytes, prymnesiophytes and a small component of diatoms. The distribution of phytoplankton communities in relation to enviromental factors is discussed in the following sections.

Cyanobacteria and Prochlorophytes

The dominances of cyanobacteria in low nutrient, high salinity waters where the N:P ratio is close to 16 is well known because smaller phytoplankton are more efficient at utilizing nutrients which allows them to thrive in oligotrophic global oceans (Ishizaka et al. 1994; Suzuki et al. 1995; Brewin et al. 2010; Hirata et al. 2011). The distinctive distribution of prochlorophytes in Cluster 4 (Fig. 2.9d) also confirmed that temperature and salinity of the KSW are critical for the existence of prochlorophytes in the ECS (Jiao et al. 2005). In our study, the presence of prochlorophytes approximately north of 32.7 ^{o}N and east of 126.5 ^{o}E, are indicative of the flow of oligotrophic Kuroshio surface water into the mid-shelf ECS.

The higher fractions of cyanobacteria in coastal, low salinity and low nutrient waters (salinity < 28, DIP < 0.2 μM, NOx < 0.5 μM) are probably comprised of *Synechococcus* which is known to be the dominant summer-time cyanobacterial species in coastal waters of the ECS (Jiao et al. 2005; Lee et al. 2014). Low nutrient concentrations resulting from strong summer stratification is considered to favor the preferential growth of small phytoplankton over the larger diatoms and dinoflagellates in coastal waters (Liu et al. 2015).

Diatoms and Dinoflagellates

In waters where DIP concentrations were high, diatoms and dinoflagellates dominated. This is evident from the results of the cluster analysis. Cluster 2 corresponded to diatom-dominated water located in the CDW and SW where salinity ranged from 28.0 to 32.9 and DIP was higher than 0.1 μM. Our observations suggest that large phytoplankton cells typically dominate the community during periods when DIP was not limiting and ExcN values were either < 0 μM or close to 0 μM (N:P = 16).

Similar findings have been reported by Hecky and Kilham (1988) for a variety of freshwater and oceanic ecosystems. Nutrient conditions akin to this, usually lead to the dominance of diatoms and dinoflagellates because of their fast growth under conditions of nutrient sufficiency (Smayda 1997).

Enhanced proportion of dinoflagellates in waters where ExcN < 0 μM shows that their nutrient requirements are close to or similar to diatoms. In all cases, however, biomass of dinoflagellates did not exceed that of diatoms. One possible reason is that dinoflagellates are less resistant to high turbulence as compared to diatoms, and easier to form blooms under stratification (Smayda 1997). Support for such a notion is based on our observations of higher concentrations of dinoflagellates in waters influenced by CDW (salinity < 30) that were less stratified. In the Changjiang Estuary and adjacent areas, high concentrations of dinoflagellates have been reported in the subsurface layer during summer with a stratified water column (Guo et al. 2014; Jiang et al. 2015).

Other Phytoplankton Groups

Highest chlorophyte populations were observed at stations which were strongly influenced by CDW with salinity < 30. In Cluster 1, the contribution of chlorophytes was more than twice that of the same in other clusters, and highly correlated with the high ExcN. In general, chlorophytes have been less investigated because they are considered minor contributors to total biomass of phytoplankton. This group has, however, been observed previously in Changjiang Estuary and in the adjacent coastal waters accounting for a sizeable fraction of CHL (Furuya et al. 2003; Zhu et al. 2009). Our study revealed the abundance of chlorophytes in the CDW when DIP concentrations were low or depleted, leading us to conclude that their distribution was linked to the spatial extent of the CDW into the mid-shelf ECS, especially when DIP was limiting, and NOx was in excess.

Prymnesiophytes accounted for more than 30% of Cluster 3, which comprised of stations mainly from SW. Prymnesiophytes are an oceanic community of phytoplankton and account for about 20% of the total primary production in central North Pacific (Rousseaux and Gregg 2013). In the ECS, prymnesiophytes have frequently been reported in offshore low CHL waters of the mid-shelf (Jiang et al. 2015; Zhu et al. 2009). *Chrysochromulina* which was found near the edge of the CDW has been reported as the dominant species (Lin et al. 2014). In the KSW, their contribution to total CHL was estimated at 20%, sharply decreasing in nearshore waters (Furuya et al. 2003) and declining to almost trace quantities in Changjiang Estuary (Liu et al. 2016; Zhu et al. 2009). The occurrence of prymnesiophytes in the ECS can be an indicator of offshore saline water intrusion into the shelf region of ECS.

2.4.2 Inter-annual variations of water mass movement and impacts on nutrient stoichiometry

The surface outflow of the Changjiang River gradually increased in salinity and decreased in nutrient concentrations, especially DIP concentrations, therefore the extent of the eastward advection and DIP-limitation of the CDW is a major factor controlling inter-annual variations of CHL in the ECS in summer (Wang et al. 2003). In our study, we found that low salinity CDW was associated with high DIN in 2010/2011 but conversely with high DIP in 2009/2013.

In 2010/2011, DIP limitation was indicated by high ExcN in the fresher CDW which created strong stratification around 124.5 ^{o}E in our study area. Such low salinity water and consequent stratification are comparable to the conditions observed further west near the Changjiang Estuary around 122 ^{o}E to 124 ^{o}E in summer (Chen et al. 2008, Tseng et al. 2014, Guo et al. 2014, Jiang et al. 2015), suggesting that CDW was less diluted by seawater during its extension into our study area in 2010/2011 (Fig. 2.3 f, g). Correspondingly, DIP concentrations in the CDW were generally < 0.2 μM, while NOx were in excess (ExcN > 0) and this led to extremely high N:P ratios (> 100) (Fig. 2.3 r, s). These results indicate that the fresher CDW could induce DIP limitation further east in the ECS in 2010/2011.

In 2009/2013, CDW with high DIP resulted in ExcN < 0. Such waters characterized Cluster 2 which showed high DIP and relatively high salinities and low temperatures. PCA analysis also showed a negative correlation between temperature and DIP. It is well known that CDW are deficient in DIP (Chen and Wang 1999; Wang et al. 2003; Chen et al. 2008), therefore high DIP in 2009/2013 in the CDW probably resulted from the mixing of CDW with subsurface nutrient-rich waters.

2.4.3 Potential mechanisms for variations in N:P ratio/ExcN

Using a three-end-member (Changjiang River plume, KIW and KSW) mixing model for the ECS, Wang et al. (2014 b) suggested that the enhanced DIP in the Changjiang River plume was from KW upwelling. An examination of surface DIP concentrations in the CDW along the two-end-member (CDW and KSW) mixing line depicts near absence of DIP in fresher (< 28.0) waters of CDW in 2010/2011 (Fig. 2.12). In the water with salinity 28.0 - 32.0, higher DIP values in excess of the two-end-member mixing line were consistently observed in 2009/2013, indicating that this offshore water of our study area had already mixed with high salinity and high DIP waters of the KIW.

Upwelling of nutrient rich KIW along the shelf slope has been suggested as a primary source of high DIP onto the ECS shelf (Ito et al. 1994; Chen et al. 1996). A branch of the KIW from the southwest of Kyushu crosses the ECS shelf (Ito et al. 1994; Guo et al. 2006). Additionally, episodic events like typhoons may cause localized upwelling on the ECS shelf and consequently some nutrient enhancement (Siswanto et al. 2008). However, the *T-S* plot and nutrient profiles for our study area did not show any indication of localized upwelling or vertical mixing, nor were any typhoon events recorded in July of the years that we sampled.

Furthermore, although nutrients of the KIW can contribute to the maintenance of a deep subsurface CHL maxima in the mid-shelf ECS (Lee et al. 2016), their influence on the offshore surface phytoplankton populations are negligible because stratification induced by the fresher CDW prevents vertical mixing of subsurface waters into the upper layers (Sukigara et al. 2017). These reasons indicate that the localized upwelling in our study area during 2009 and 2013 was not responsible for supplying DIP-rich waters to the surface layers.

Instead we propose that intensive nearshore wind driven coastal upwelling brings DIP-rich water upward and then mixes with near surface CDW. It is known that the coastal upwelling induces high primary production from replenishment of DIP in summer in the ECS (Gong et al. 1996; Chen et al. 2004; Wang and Wang 2007). Under the influence of the strong southwesterly monsoon, colder upwelled DIP-rich water has been often observed along the coast of China because of mixing of the Changjiang water with subsurface waters of the Taiwan Warm Current or the KIW (Chen et al. 2004; Yang et al. 2013). Furthermore, additional DIP can be supplied by the remineralization of organic matter in the bottom waters (Gong et al. 1996; Fang et al. 2004; Yang et al.

2013).

Previous studies (Liu et al. 2013; Tseng et al. 2014) reported extensive phytoplankton blooms triggered by coastal upwelling around Changjiang Estuary and which often extend eastward to 123 ^{o}E. These blooms result in DIP limitation in the plume fringe where salinity > 30. We observed CDW with salinity of 30 extending up to 124.5 ^{o}E in 2009/2013, and coincident with location plume fringe in the afore mentioned studies. This result is also consistent with the conclusion of Tseng et al. (2014) that the magnitude of phytoplankton blooms and DIP-limitation outside of the Changjiang Estuary determined by the joint effect of CDW and coastal upwelling.

Here we extend this coastal upwelling hypothesis of Tseng et al. (2014) to explain the interannual variations in phytoplankton community in response to varying N:P ratios in the CDW (Fig. 2.13). If the CDW is highly stratified (salinity < 28 in our study) suppressing near surface water mixing with subsurface water, then surface DIP is rapidly consumed by phytoplankton in the outer Changjiang Estuary. This results in DIP-limitation and the dominance of smaller phytoplankton, such as cyanobacteria as observed in 2010/2011 during our study (Fig. 2.13 a). On the other hand, when intensive coastal upwelling occurs, it brings high-DIP subsurface water upward which mixes with the surface CDW around Changjiang estuary. The resulting CDW with low N:P ratio advected eastward, and sustained the growth of larger phytoplankton, such as diatoms and dinoflagellates, in offshore waters (Fig. 2.13 b) as observed in 2009/2013 during our study.

Zhang et al. (2007) have also reported that low N:P surface waters around Changjiang Estuary were the result of low N:P ratio (< 10) subsurface and intermediate water masses affected by the DIP-rich Kuroshio waters. Similarly, we also observed N:P < 10 in bottom waters at CDW stations (Fig. 2.2 c, d). It thus appears that the combined effect of CDW and coastal upwelling is important in determining the inter-annual variability of nutrient concentrations and consequently phytoplankton community in the mid-ECS shelf.

Intensive coastal upwelling in 2009 and 2013 was indicated by sea surface temperature (SST) anomalies and a northward wind pattern along the coast of China (Fig. 2.S1). However, large scale hydrological and biogeochemical studies are necessary to shed light on the inter-annual variations in the interaction of Changjiang river plume and coastal upwelling both of which drive nutrient inputs into the ECS shelf region, and consequently determine the phytoplankton community structure and the overall biogeochemical cycling within the ECS.

2.5 Conclusions

Our study is the first to document inter-annual variations in the phytoplankton community of the mid-shelf ECS in relation to the nutrient stoichiometry resulting from variations in the water masses of the ECS. Compared to the low nutrient concentrations and invariant N:P ratios that typified the Kuroshio waters, significant differences in water properties and nutrient concentrations were observed in the CDW influenced region during the four summers of sampling. DIP concentrations in the CDW were low in 2010/2011, but it was remained in 2009/2013. As a result, mixed populations of phytoplankton were observed in 2010/2011 while diatom domination was observed in 2009/2013. This study shows that DIP supply is crucial in determining the phytoplankton composition in the mid-shelf ECS. Compared to the highly stratified CDW in 2010/2011, CDW in 2009/2013 was in all probability already mixed with the upwelled subsurface waters from the coastal region supporting a more eastward dispersal of high phytoplankton concentrations into the mid-shelf ECS over longer time periods.

Table 2.1. Initial and final ratios of pigments to chlorophyll *a* (CHL) of nine phytoplankton groups used in the CHEMTAX analysis. Abbreviations: CHL: Chlorophyll *a*, fucox: fucoxanthin, perid: peridinin, 19butfu: 19'-butanoyloxyfucoxanthin, 19hexfu: 19'-hexanoyloxyfucoxanthin, zeax: zeaxanthin, Chlb: Chlorophyll *b*, neox: neoxanthin, violax: violaxanthin, allox: alloxanthin, prasinox: prasinoxanthin, DV-Chla: divinyl-chlorophyll *a*. Prochlorophyte were excluded from cyanobacteria.

Initial ratio												
Group/ Pigment	perid	19butfu	fucox	19hexfu	neox	prasinox	violax	allox	zeax	Chlb	DV-Chla	CHL
Prasinophytes	0	0	0	0	0.11	0.36	0.11	0	0	0.89	0	1
Dinoflagellates	0.53	0	0	0	0	0	0	0	0	0	0	1
Cryptophytes	0	0	0	0	0	0	0	0.14	0	0	0	1
Prymnesiophytes	0	0	0	1.4	0	0	0	0	0	0	0	1
Chrysophytes	0	0.93	0.62	0	0	0	0	0	0	0	0	1
Chlorophytes	0	0	0	0	0.04	0	0.03	0	0.06	0.28	0	1
Cyanobacteria	0	0	0	0	0	0	0	0	0.33	0	0	1
Diatoms	0	0	0.75	0	0	0	0	0	0	0	0	1
Prochlorophytes	0	0	0	0	0	0	0	0	0	0	1	0
												2009
Final ratio												
Group/ Pigment	perid	19butfu	fucox	19hexfu	neox	prasinox	violax	allox	zeax	Chlb	DV-Chla	CHL
Prasinophytes	0	0	0	0	0.11	0.21	0.08	0	0	1.15	0	1
Dinoflagellates	0.78	0	0	0	0	0	0	0	0	0	0	1
Cryptophytes	0	0	0	0	0	0	0	0.16	0	0	0	1
Prymnesiophytes	0	0	0	1.4	0	0	0	0	0	0	0	1
Chrysophytes	0	0.93	0.62	0	0	0	0	0	0	0	0	1
Chlorophytes	0	0	0	0	0.03	0	0.10	0	0.10	0.28	0	1
Cyanobacteria	0	0	0	0	0	0	0	0	1.39	0	0	1
Diatoms	0	0	0.49	0	0	0	0	0	0	0	0	1
Prochlorophytes	0	0	0	0	0	0	0	0	0	0	1	0
												2010
Final ratio												
Prasinophytes	0	0	0	0	0.09	0.25	0.19	0	0	0.60	0	1
Dinoflagellates	0.53	0	0	0	0	0	0	0	0	0	0	1
Cryptophytes	0	0	0	0	0	0	0	0.14	0	0	0	1
Prymnesiophytes	0	0	0	1.4	0	0	0	0	0	0	0	1
Chrysophytes	0	0.93	0.62	0	0	0	0	0	0	0	0	1
Chlorophytes	0	0	0	0	0.01	0	0.02	0	0.05	0.27	0	1
Cyanobacteria	0	0	0	0	0	0	0	0	0.52	0	0	1
Diatoms	0	0	0.68	0	0	0	0	0	0	0	0	1
Prochlorophytes	0	0	0	0	0	0	0	0	0	0	1	0
												2011
Final ratio												
Prasinophytes	0	0	0	0	0.14	0.33	0.04	0	0	0.98	0	1
Dinoflagellates	0.72	0	0	0	0	0	0	0	0	0	0	1
Cryptophytes	0	0	0	0	0	0	0	0.59	0	0	0	1
Prymnesiophytes	0	0	0	0.66	0	0	0	0	0	0	0	1
Chrysophytes	0	0.93	0.62	0	0	0	0	0	0	0	0	1
Chlorophytes	0	0	0	0	0.01	0	0.003	0	0.04	0.27	0	1
Cyanobacteria	0	0	0	0	0	0	0	0	0.69	0	0	1
Diatoms	0	0	0.61	0	0	0	0	0	0	0	0	1
Prochlorophytes	0	0	0	0	0	0	0	0	0	0	1	0
												2013
Final ratio												
Prasinophytes	0	0	0	0	0.11	0.36	0.11	0	0	0.89	0	1
Dinoflagellates	0.46	0	0	0	0	0	0	0	0	0	0	1
Cryptophytes	0	0	0	0	0	0	0	0.14	0	0	0	1
Prymnesiophytes	0	0	0	0.30	0	0	0	0	0	0	0	1
Chrysophytes	0	0.93	0.54	0	0	0	0	0	0	0	0	1
Chlorophytes	0	0	0	0	0.08	0	0.02	0	0.13	1.82	0	1
Cyanobacteria	0	0	0	0	0	0	0	0	1.20	0	0	1
Diatoms	0	0	0.42	0	0	0	0	0	0	0	0	1
Prochlorophytes	0	0	0	0	0	0	0	0	0	0	1	0

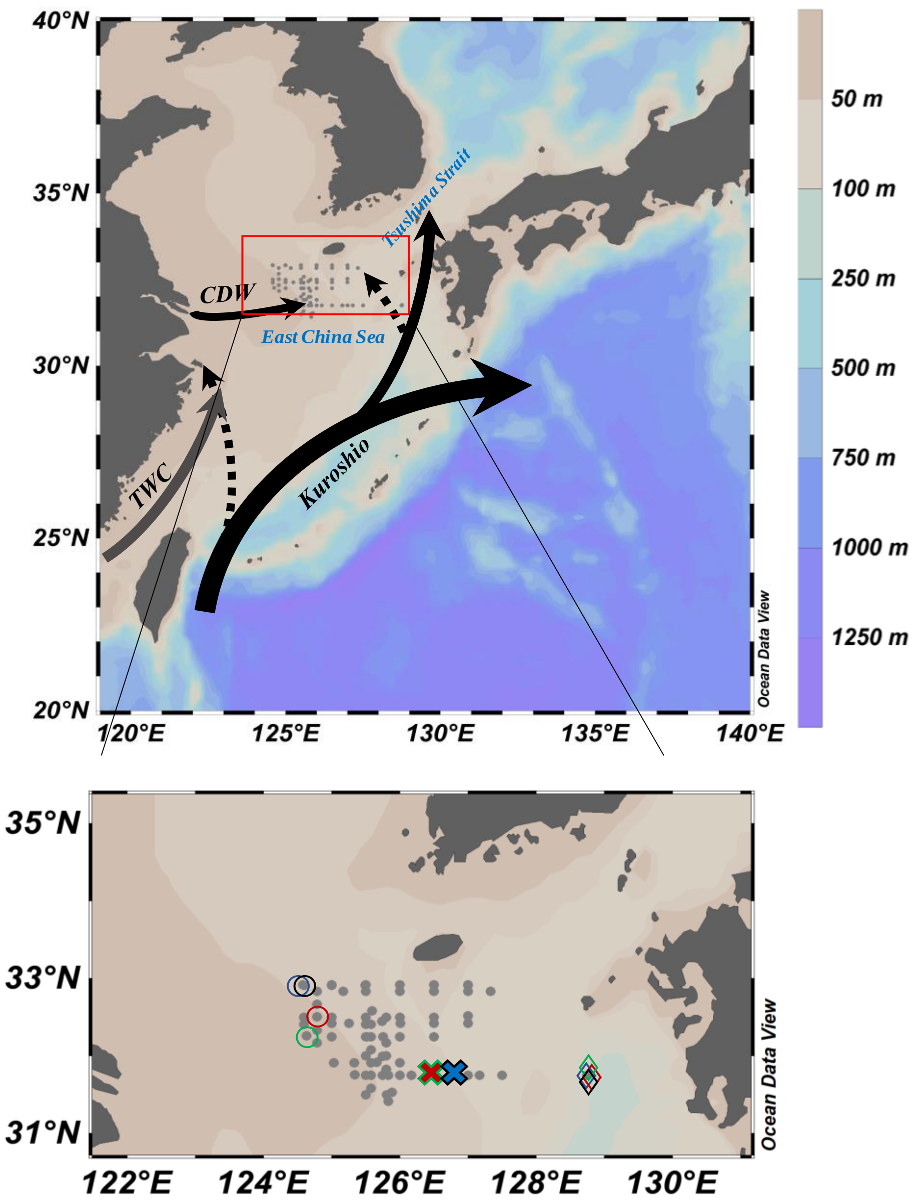

Fig. 2.1. Sampling locations for four cruises in the mid-shelf East China Sea undertaken in late July of 2009-2011 and 2013. One of CDW (circles), SW(crosses) and KSW (diamonds) stations in 2009 (black), 2010 (blue), 2011 (green) and 2013 (red) were selected to compare T-S diagrams and vertical profiles of nutrients in different years shown in Figure 2. Surface currents are indicated by solid lines and include the Kuroshio, Changjiang Diluted Water (CDW), Taiwan Warm Current (TWC). Two pathways of Kuroshio intrusion; one from the northeast of Taiwan and the other towards the southwest of Kyushu are indicated by dashed lines.

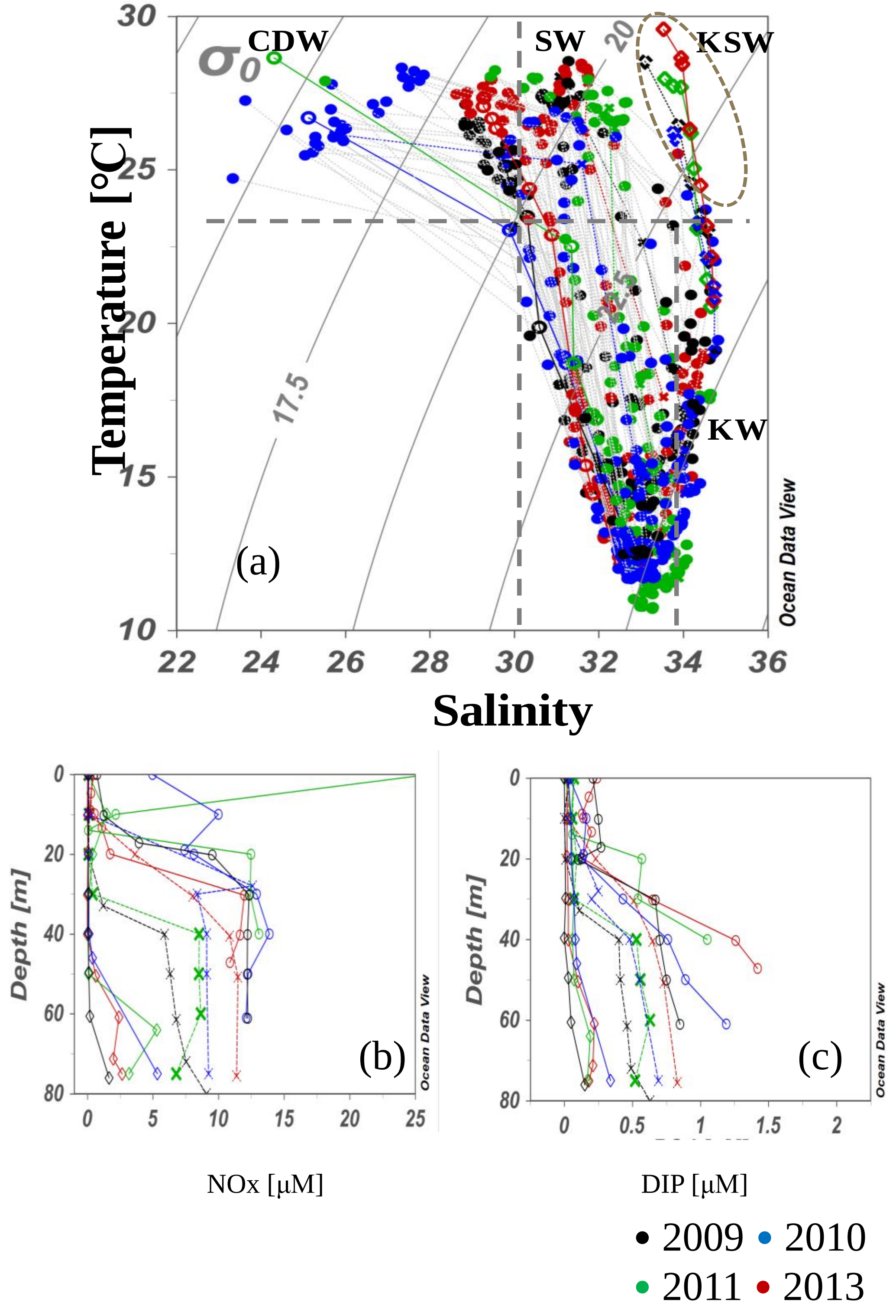

Fig. 2.2. Temperature-salinity (*T-S*) plot of the upper 80 m depth delineating water masses described in this study (a). Vertical profiles of NOx (b) and DIP (c) at selected stations in KSW (diamonds), SW(crosses) and CDW (circles).

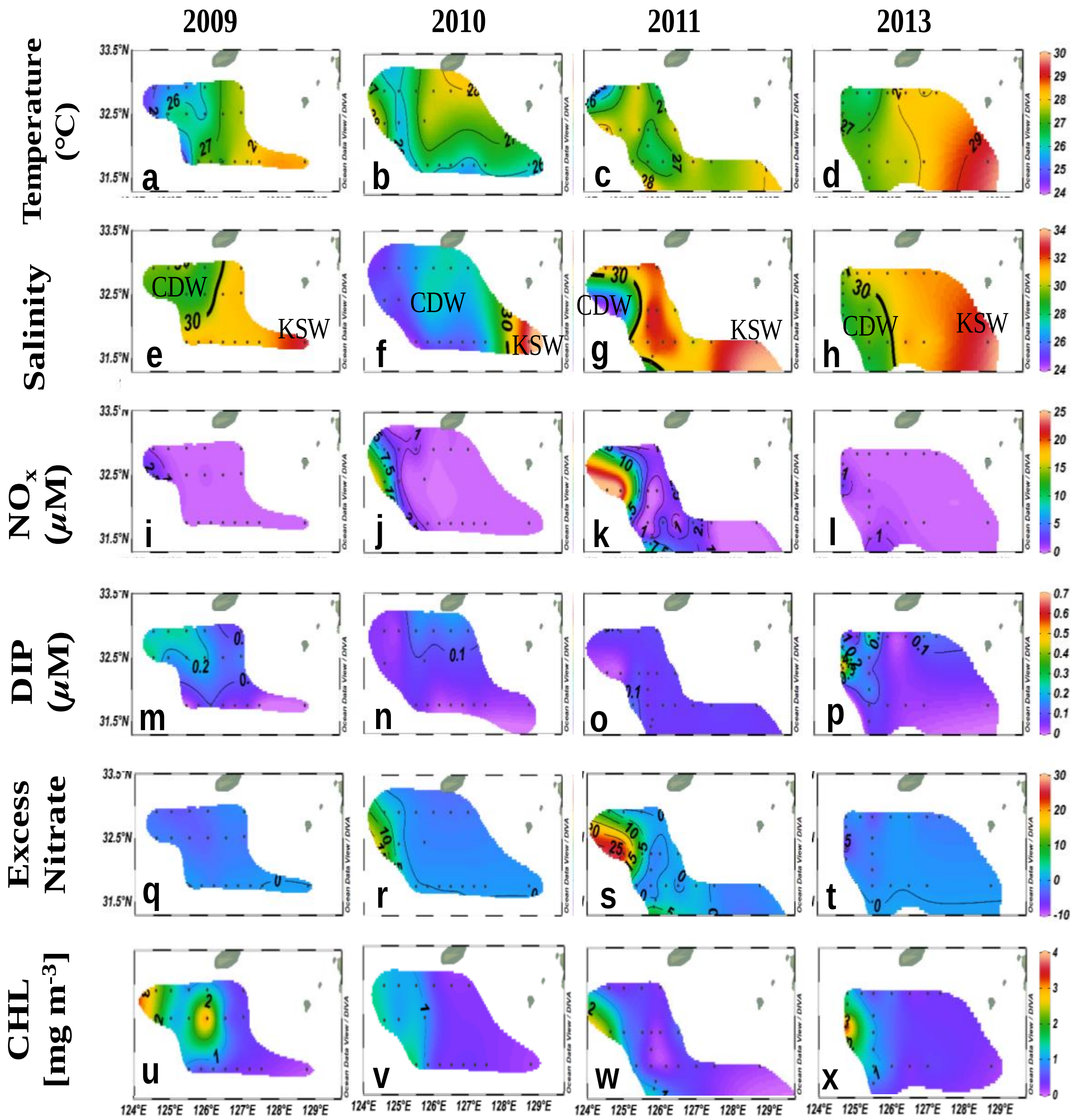

Fig. 2.3. Distributions of surface temperature (a - d), salinity (e - h), NOx (i - l), DIP (m - p), excess nitrate (q - t), and CHL (u - x) in 2009 - 2011 and 2013. Black dots are sampling stations.

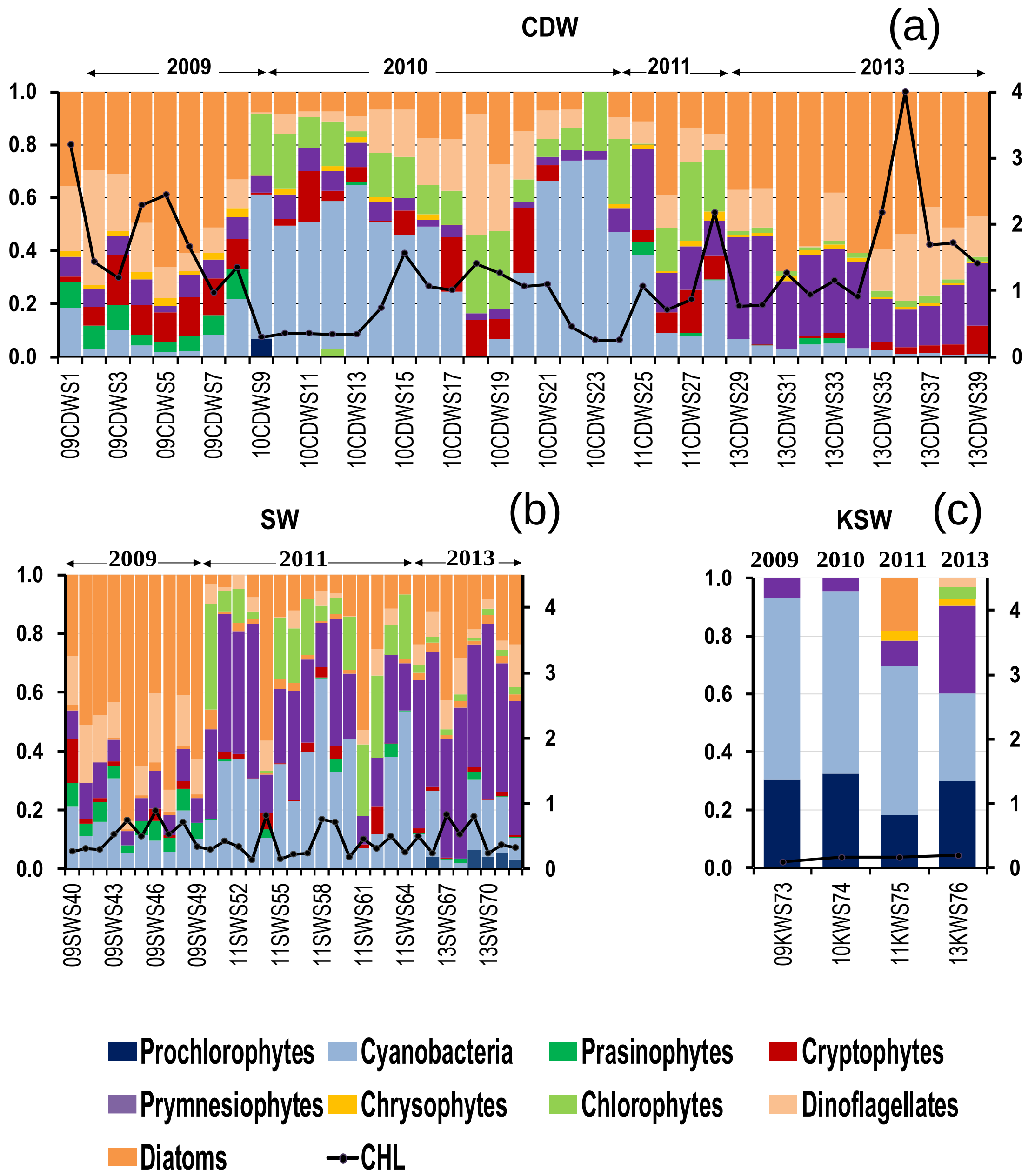

Fig. 2.4. CHL concentrations and phytoplankton communities estimated by HPLC pigment analysis and CHEMTAX in the three water masses (a: CDW, b: SW and c: KSW) in 2009 - 2011 and 2013.

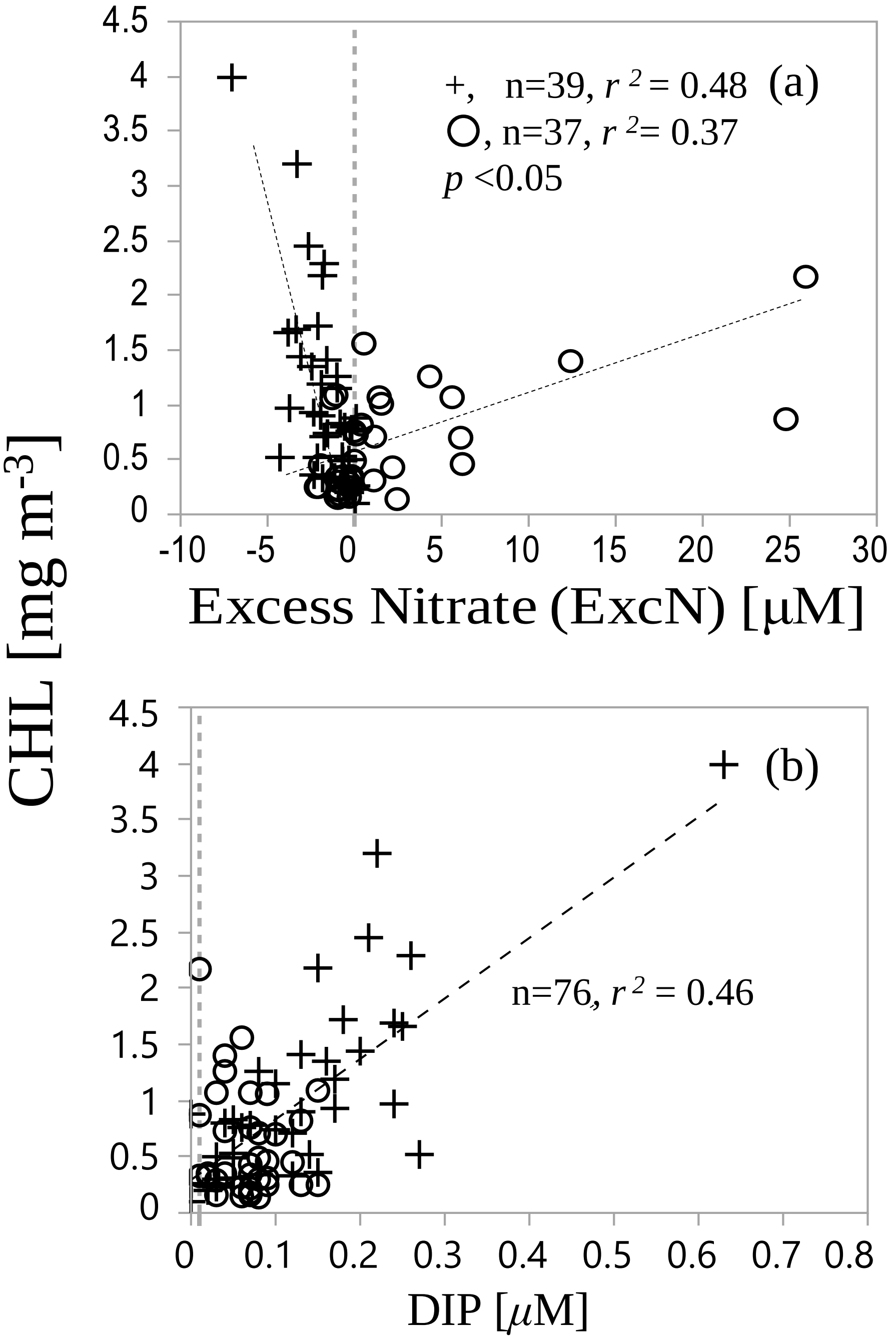

Fig. 2.5. (a) CHL concentration versus Excess Nitrate (ExcN) in high-DIP-years (+) and high-NOx-years (○). (b) CHL concentration versus DIP in the surface East China Sea for all four years. $p < 0.05$ indicates that CHL was significantly different between high-DIP-year (+) and high-NOx-year (○). Dashed grey lines in (a) indicated N:P = 16, in (b) indicated the detection limit of DIP (0.01 μM).

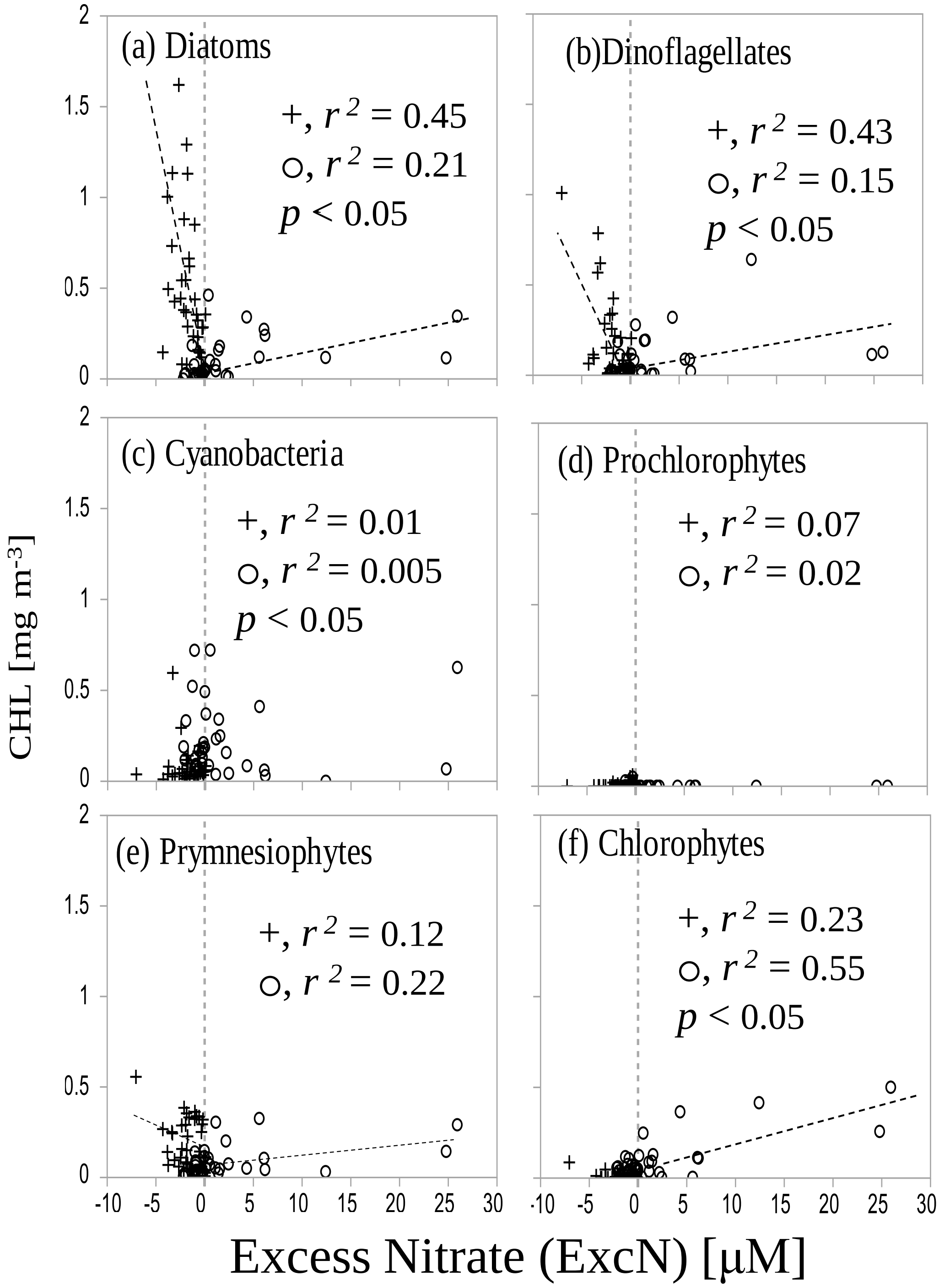

Fig. 2.6. Abundance of phytoplankton communities versus Excess Nitrate (ExcN) in the surface ECS during high-DIP-year (+) and high-NOx-year (○). $p < 0.05$ indicates that phytoplankton concentration was significant different between high-DIP-year (+) and high-NOx-year (○).

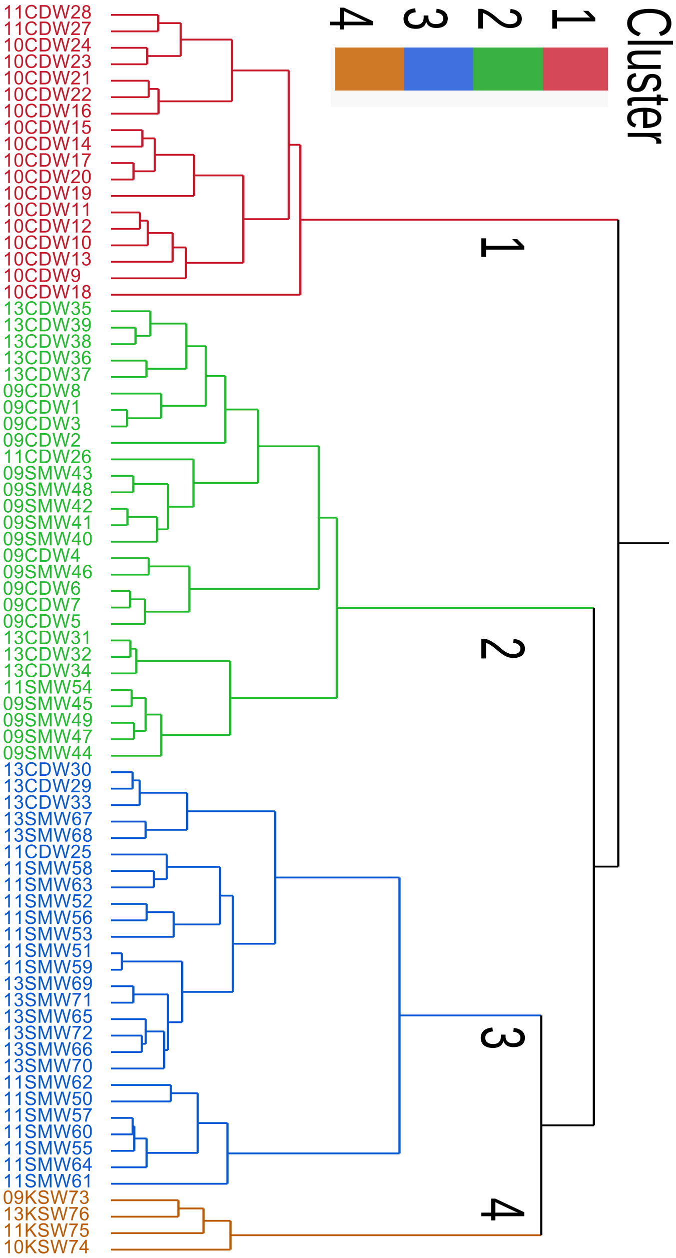

Fig. 2.7. Dendrogram of cluster analysis based on phytoplankton composition.

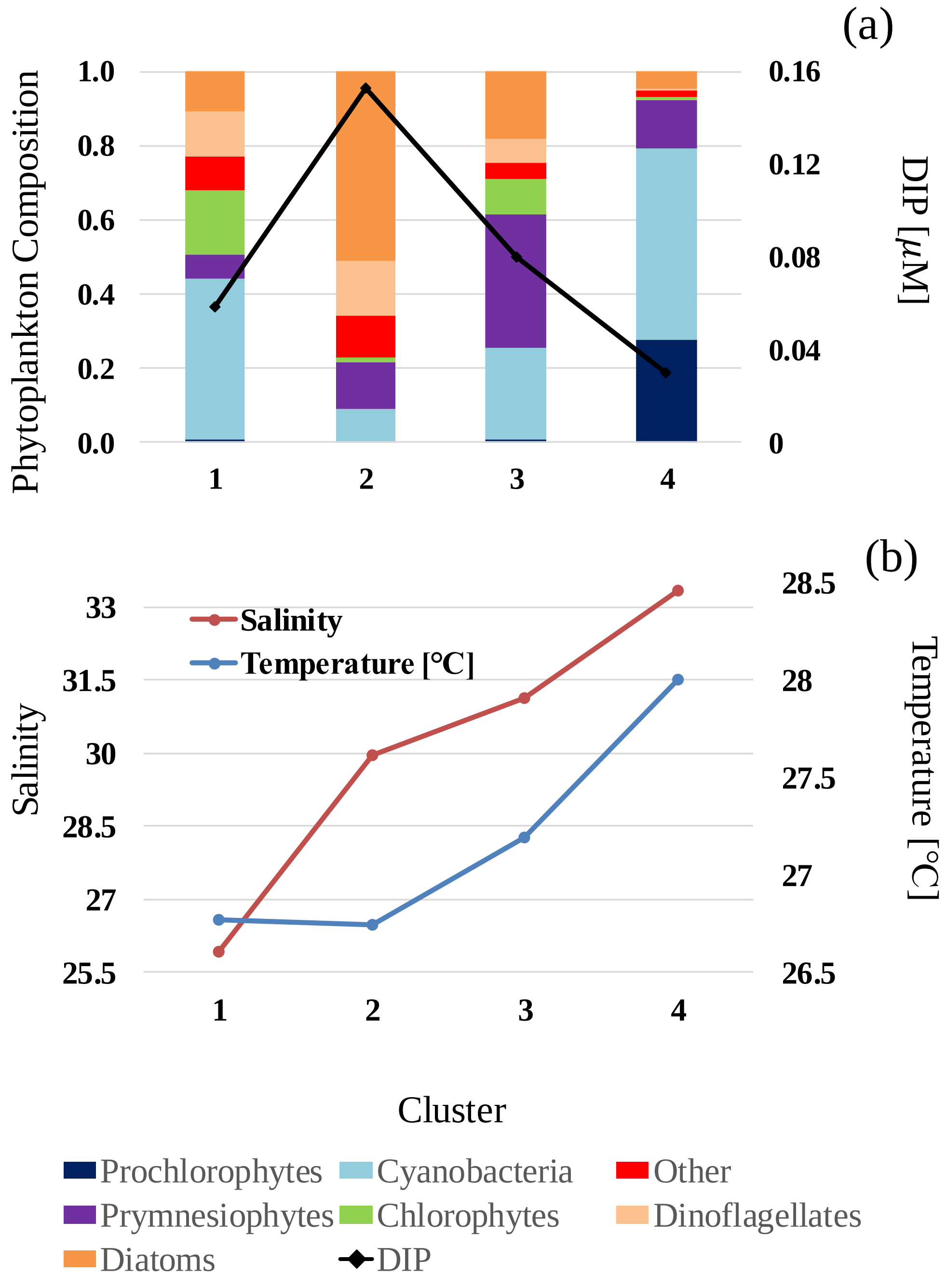

Fig. 2.8. Averaged values of surface phytoplankton composition and DIP (a) and temperature and salinity (b) in each cluster in the mid-shelf of the ECS. Black line indicates averaged DIP concentration.

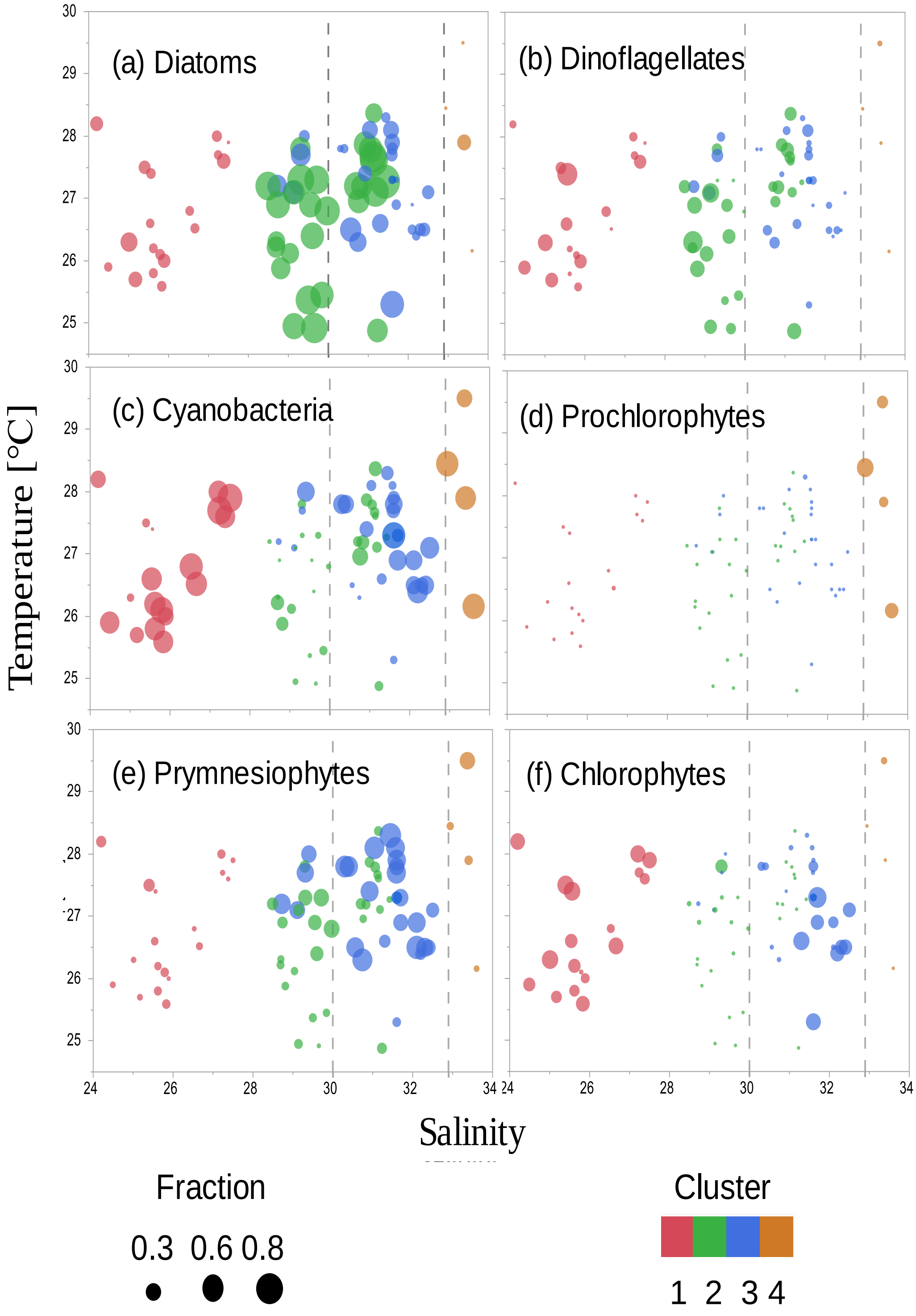

Fig. 2.9. Relative abundances of surface phytoplankton communities in *T-S* plots in the ECS for the four years. Clusters are indicated by different colors. Dashed lines divide water masses according to salinity as CDW (< 30), SW (30 - 32.9) and KSW (> 32.9).

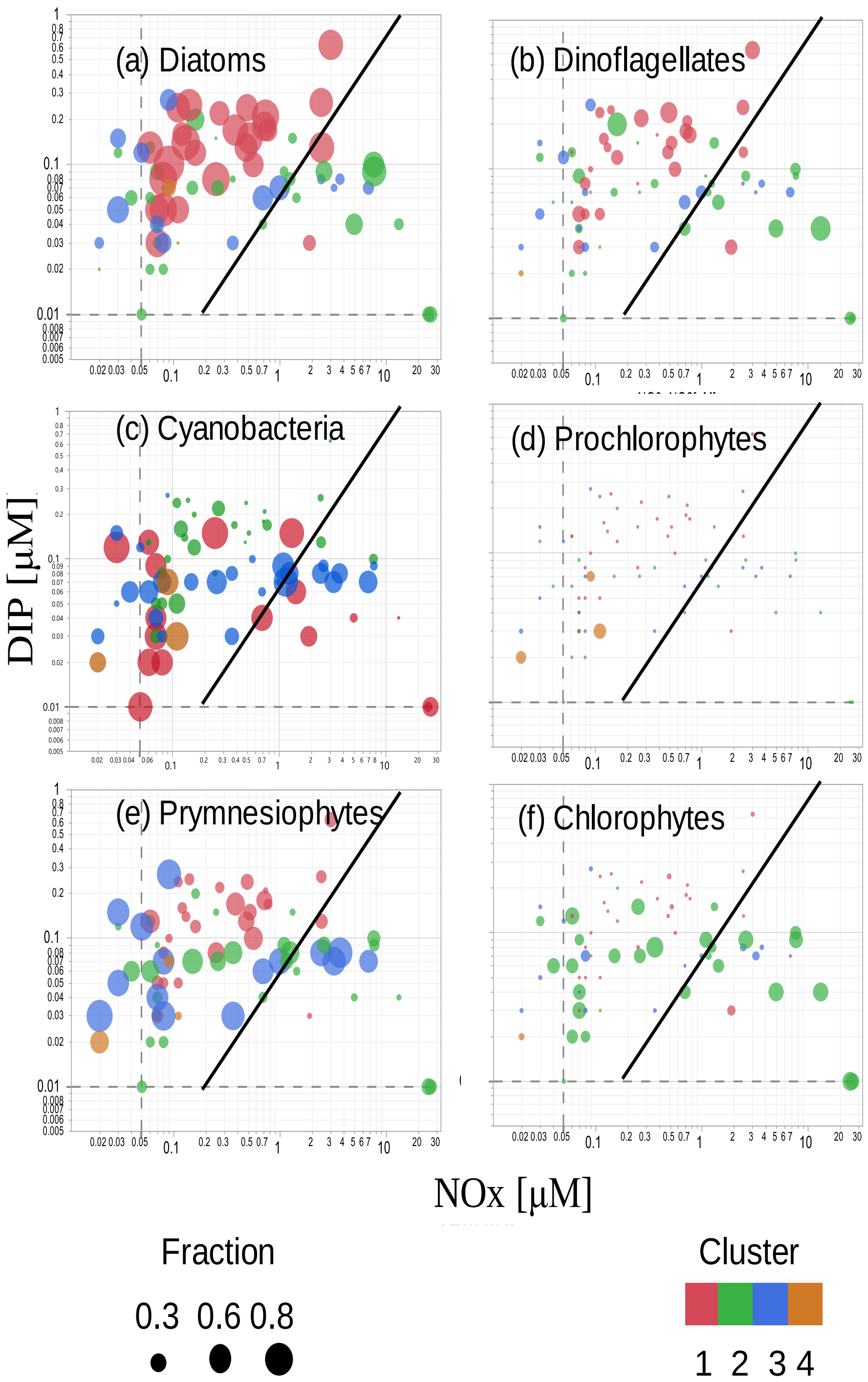

Fig. 2.10. Relative abundances of surface phytoplankton communities in DIP-NO_x plots in the East China Sea for four years. Clusters are indicated by different colors. Dashed lines indicated detection limit of nutrients (DIP: 0.01 μM, NO_x: 0.05 μM). Solid line indicates N:P =16.

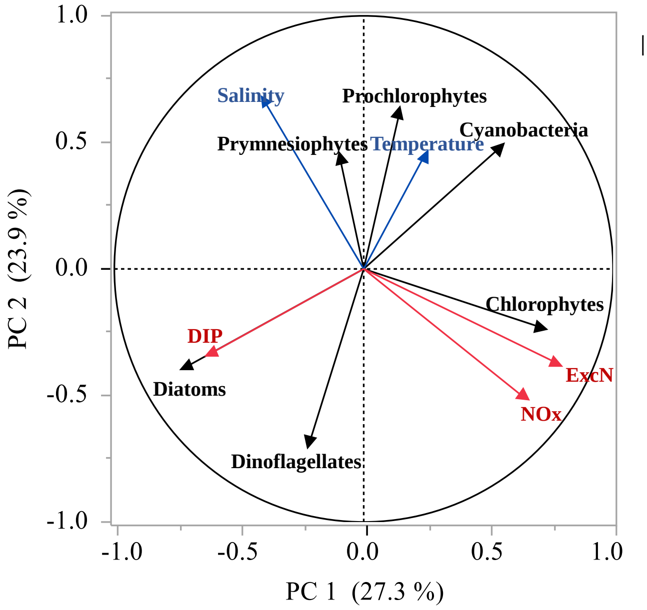

Fig. 2.11. Principal Component Analysis of the phytoplankton composition and environmental factors in the ECS. Colors of vectors: black indicate phytoplankton, blue indicates physical parameters, and red indicates chemical parameters.

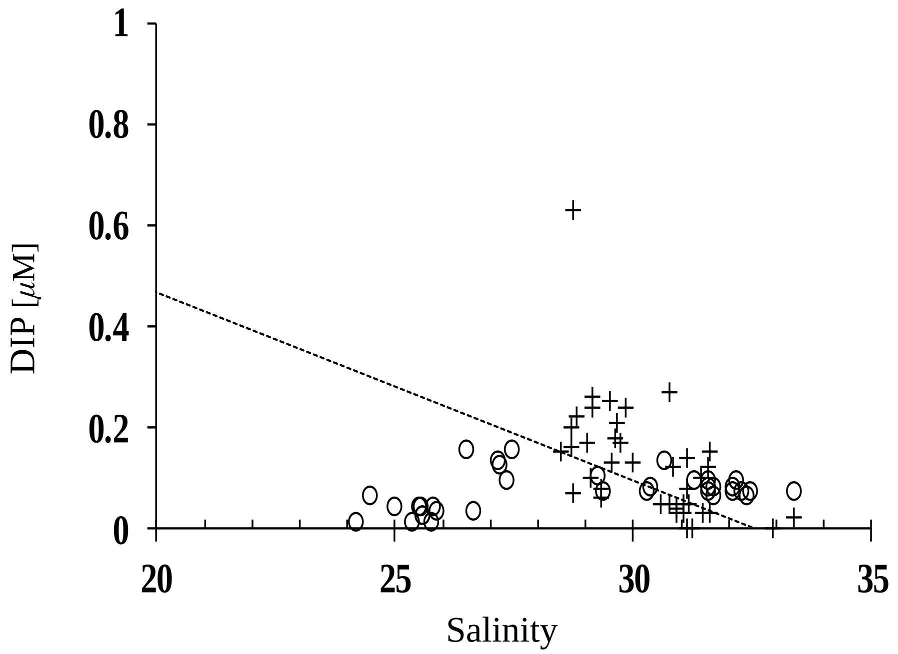

Fig. 2.12. Relationship between surface DIP and salinity for all stations in this study; (+) 2009/2013 and (○) 2010/2011. The dotted line is obtained from Zhang et al. (2007).

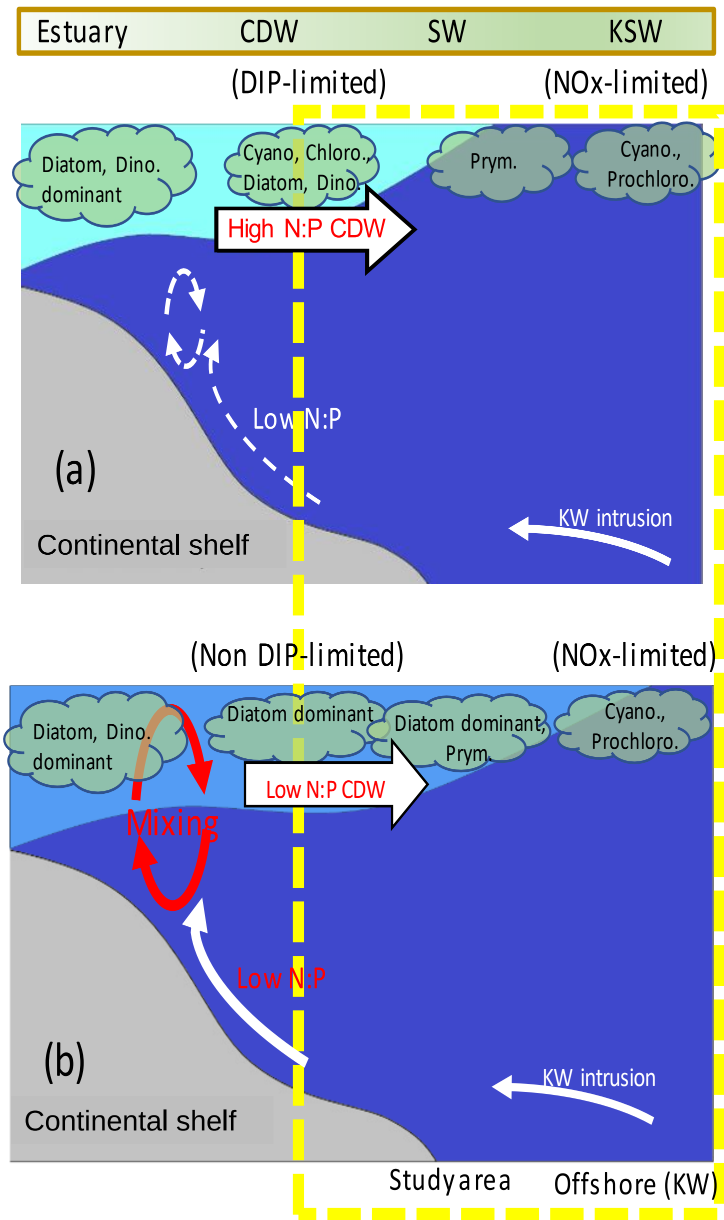

Fig. 2.13. Schematic of interannual variation of summer phytoplankton community distribution in the ECS; (a) Mixed populations of cyanobacteria, chlorophytes, diatoms and dinoflagellates exist in DIP limited water as a result of high N:P ratio of the CDW (cf. 2010/2011), (b) Diatom dominates in no-DIP-limited water resulted by mixing of CDW with low N:P upwelled water near the coast (cf. 2009/2013). Dino.: dinoflagellates, Chhloro.: chlorophytes, Cyano.: cyanobacteria, Prym.: prymnesiophytes, Prochloro.: prochlorophytes.

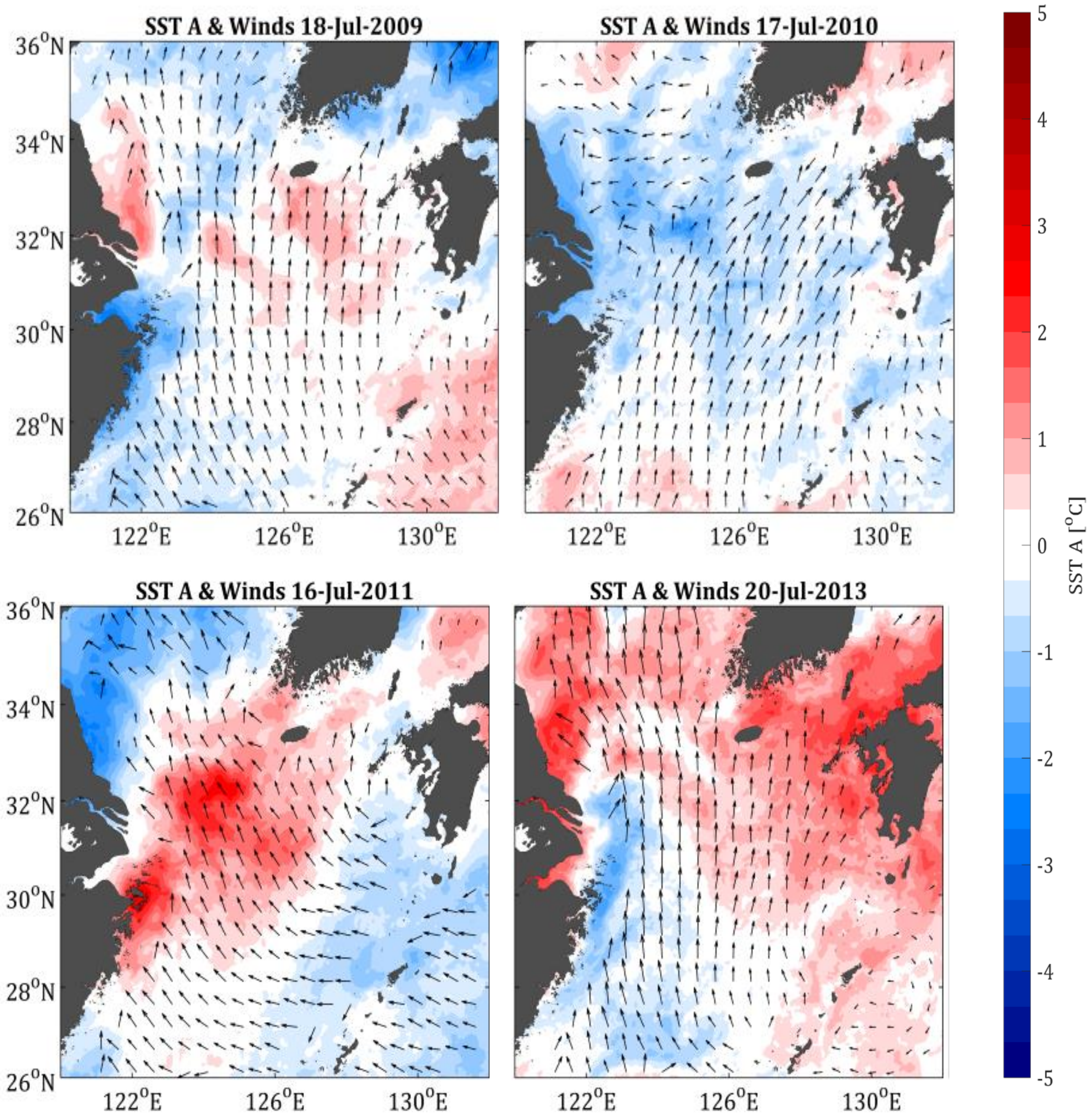

Fig. 2.S1. Weekly Sea Surface Temperature anomaly (SST A) (https://mur.jpl.nasa.gov/) calculated from weekly SST, and overlaid with weekly wind intensity (arrows) (http://www.remss.com/) in the third week of July 2009, 2010, 2011 and 2013.

Chapter3 High-resolution vertical observations of phytoplankton groups derived from an *in situ* fluorometer in the East China Sea and Tsushima Strait

3.1 Introduction

Phytoplankton communities determine the structure and function of marine ecosystems and changes in phytoplankton community structure in response to physical and chemical environments have direct effects on higher trophic levels and biogeochemical cycling in the ocean (Simpson and Sharples, 2012; Goes et al. 2014). The East China Sea (ECS) is influenced by the third largest river in the world, the Changjiang River which discharges waters with high anthropogenic inputs from human activities (Zhang et al., 2007). In the mid-shelf ECS, fingerprints of the Changjiang River Diluted water (CDW) can be observed from its high dissolved inorganic nitrogen (DIN) content, and Redfield ratios exceeding 100, because dissolved inorganic phosphate (DIP) is rapidly consumed by phytoplankton blooms at the mouth of the Changjiang Estuary (Wang and Wang 2007; Chen 2008). In the ECS, DIP is generally limiting for diatoms and dinoflagellates growth (Wang et al., 2014, Liu et al., 2016) but this is occasionally ameliorated by coastal upwelling induced by Kuroshio intrusion that alters nutrient concentrations in the CDW, and consequently phytoplankton composition

(Xu et al., 2018, Gomes et al., 2018, Ishizaka et al., 2021).

Satellite based ocean color images reveal the large seasonal and spatial variability of chlorophyll a (CHL) concentrations in the ECS in association with the movement of the CDW, with high phytoplankton concentrations (CHL > 60 mg m^{-3}) observed in the Changjiang estuary and adjacent areas, but which is drastically reduced (< 1 mg m^{-3}) in the outer shelf in summer (Yamaguchi et al. 2012; 2013). Separation of phytoplankton pigments using High-performance liquid chromatography (HPLC) and pigment-based identification of major phytoplankton groups (Mackey et al., 1996; Jeffrey and Vesk 1997, Wright, 2005) have been used to characterize phytoplankton community structure limitations posed by laborious water sampling and HPLC pigment separation, which results in data obtained from only a few depths, hampering a thorough understanding of fine-scale changes in phytoplankton structure with depth specifically in the East China Sea (Ishizaka et al., 2021). For the ECS, this limitation of data in the vertical persists to this day.

A submersible multiple excitation fluorometer, FluoroProbe (bbe moldaenke, Germany), introduced by Beutler et al. (2002a), showed that it is possible to get high resolution of phytoplankton communities with depth, thus alleviating the limitations posed by discrete depth water sampling. These fluorometers take advantage of the differences in pigments that characterize various phytoplankton groups especially the pigment biomarkers that have been used to determine phytoplankton functional groups (Wright and Jeffrey 2006, Uitz et al., 2015). Phytoplankton pigments absorb light in various wavelengths and thus enable the separation of phytoplankton groups based on their specific fluorescence excitation spectra. FluoroProbe measures CHL fluorescence emission at 685nm with excitation at five wavelengths (450, 525, 570, 590, and 610 nm) (Beutler et al., 2002). The fraction of the four phytoplankton groups (a brown group comprising of diatoms and dinoflagellates; a blue group of cyanobacteria; a green group comprising of chlorophytes; a mixed group comprising of cryptophytes) can then be calculated according to the spectral shapes (Beutler et al., 2002). The FluoroProbe has showed the ability to detect phytoplankton groups in a rapid and automated way in several freshwater ecosystems (Ghadouani and Smith 2005; Rolland et al 2010, Alexander et al 2012).

Recently, a smaller, more compact and a more economical alternative, Multi-Exciter fluorometer (JFE Advantech, Japan) that operates on the sample principle as the FluoroProbe, has been developed (Pires 2010, Yamamoto et al., 2021). Multi-Exciter has nine excitation wavelengths (375, 400, 420, 435, 470, 505, 525, 570, and 590 nm) and can its software can separate three phytoplankton groups (brown algae, cyanobacteria, and green algae) (Yoshida et al., 2011). It showed great capability to capture changes in pigment composition with environmental changes in the Arctic

(Fujiwara et al., 2018). However other studies especially in coastal waters, found that this instrument performed poorly with low accuracies and large errors (See et al 2005; Liu et al., 2012). To resolve this problem, a model was developed to calibrate the fluorometer with in-situ HPLC pigment data, and then estimate phytoplankton groups from fluorescence excitation spectra. This model provided significant improvements in estimating phytoplankton groups even in coastal waters (Wang et al., 2016).

In this study, we have made use of multiple excitation fluorometer data calibrated with in-situ HPLC pigment data, to describe the horizontal and vertical distribution of phytoplankton in relation to environmental factors in the ECS (including the Kuroshio region) and TS in summer. By taking the advantage of high-resolution vertical profiles of the phytoplankton community estimated by a multiple excitation fluorometer, we were able to observe clear variations in phytoplankton community structure in response to different water mass properties.

3.2 Data and Methods

Water sampling and satellite observations

In-situ sampling was undertaken in the ECS and the Tsushima Strait (TS) during cruises on board the T/V *Nagasaki Maru* in July of 2011 - 2014 (Fig.3.1). At each station, a CTD profiler with Niskin bottles was used to conduct hydrographic measurements and water sampling. Water was sampled from 2-4 layers which included the surface, subsurface chlorophyll *a* maximum (SCM), above the SCM and below the SCM.

Surface water samples for CHL, phytoplankton pigments and nutrients (including DIN = NO_3^- + NO_2^-, DIP: PO_4^{3-}) were collected using an acid-washed bucket. Nutrient samples were immediately frozen in polyethylene tubes and transferred under frozen conditions to the shore laboratory for analysis using an Auto-analyzer (AACS-IV, BLTEC). DIN and DIP concentrations were determined according to absorption spectrometry (Armstrong et al. 1967, Murphy and Riley 1961, Koroleff 1983). The observation area in 2013 was overlapped with 2011, therefore three transects (ECS-2011, TW-2012 and KW-2014) in the featured region were selected to show the differences in regional water mass properties and phytoplankton communities of the euphotic water column (Fig.3.1).

Sea surface temperature (SST) and MODIS/Aqua CHL were obtained from the NASA Ocean Color website (http://oceancolor.gsfc.nasa.gov/). Monthly composites for our study area (122-132^{o}N, 28-36^{o}E), for July 2011, 2012 and 2014 were extracted from global coverage datasets.

Estimation of phytoplankton communities from pigment concentration

Water samples for HPLC pigment analysis (1 - 2 L) were filtered on to 25mm Whatman GF/F glass fiber filters under a vacuum pressure (< 0.01 MPa) and dim light, immediately frozen in liquid nitrogen for measurement in the laboratory. Concentrations of 19 pigments were measured by KANSO CO., LTD according to the method of Van Heukelem & Thomas (2001) using reverse-phase HPLC with a Zorbax Eclipse XDB-C8 column (150 mm × 4.6 mm, 3.5 μm; Agilent Technologies).

CHEMTAX was used to interpret phytoplankton group composition based on pigment data. Matrices of pigment data and initial pigments/CHL ratio for each phytoplankton group were used as input of the CHEMTAX program (Mackey et al 1996). Thirteen marker pigments were selected and classified into nine phytoplankton groups according to published papers in the ECS and adjacent areas (Furuya et al 2003, Zhu et al., 2009, Liu et al, 2016). Samples were separated into different subsets according to their similarity of pigment compositions by clustering analysis to ensure the pigment ratios were constant for CHEMTAX analysis. For each dataset, CHEMTAX program was run 10 times by using the output ratio matrix of the last run as the next ratio matrix input and the optimized phytoplankton compositions were selected from the most stable final ratios among the 10 outputs (Latasa 2007). More details on deriving the appropriate proportions of phytoplankton groups from CHL, using the CHEMTAX program are described in detail in our earlier work (Gomes et al., 2018).

Estimation of phytoplankton communities from fluorescence excitation spectra

After vertical profiles of phytoplankton excitation spectra were collected using the Multi-Exciter, the model of Wang et al. (2016) was applied to estimate phytoplankton groups from measured the fluorescence spectra. In brief, this model includes three steps: 1) Continuum removal and band ratio were processed to obtain spectral features from phytoplankton fluorescence excitation spectra *F(λ)* which are associated with the composition of phytoplankton groups. 2) Principle component analysis (PCA) was used to compress the redundancy of spectral features and to obtain PC scores, which were used to derive the CHL fractions of the phytoplankton groups. 3) A sigmoid function was used to estimate phytoplankton groups from spectral data as;

$$f = \frac{1}{1+exp[-(c_0+\sum_{i=1}^{k} c_i S_i)]} \tag{1}$$

where *f* denotes CHL fractions of brown algae, cyanobacteria, or green algae; *Si* is the *i*-th PC score; *c0* and *ci* are regression coefficients between phytoplankton group fractions and PC scores (*Si*); *k* is the number of PCs, which was set to 8 because 99% of the variance of the original dataset can be explained by the first 8 PC scores.

In this study, four groups were determined according to the spectral characteristics of each group (brown algae, cyanobacteria, green algae and cryptophytes). The upper and lower limits of *f* were set as 1 and 0 respectively to avoid unrealistic estimates.

Cryptophytes were calculated as $1-f_{brown\ algae}-f_{cyanobacteria}-f_{green\ algae}$ by considering that the sum of four phytoplankton groups is 1. More details of the model can be found in Wang et al. (2016). Datasets from 2011 to 2013 are from Wang et al. (2016) which after calibration, showed statistically high relationships with CHEMTAX derived phytoplankton groups (R^2 = 0.64, 0.68, 0.36 and 0.49 and RMSE = 0.117, 0.078, 0.072 and 0.060 for brown algae, cyanobacteria, green algae and cryptophytes, respectively). Data from 2014 was recalibrated with HPLC samples collected that year to improve the accuracy of the model. Correlation coefficients (R^2) varied from 0.72, 0.87, 0.61 and 0.19 and RMSE were less than 0.2 for brown algae, cyanobacteria, green algae and cryptophytes, respectively.

3.3 Results

3.3.1 Water mass properties

Surface SST and CHL

Satellite imagery were used to compare interannual variations in SST and CHL in the ECS and TS in July during three years. SST was higher than 30 ^{o}C at low latitudes around 32 ^{o}N and decreased to less than 25 ^{o}C, north of 34 ^{o}N during all three years (Fig. 3.2 a - c). High SST during each year was associated with the pathway of Kuroshio current flowing southeast of the ECS. In the region influenced by the Kuroshio, SST varied only slightly over the three years, but relatively higher temperatures and wider ranges were observed south of Kyushu Island in 2012 (Fig. 2 b). Along the Chinese coast, high temperature water (> 30 ^{o}C) was observed nearshore, in the Changjiang Estuary, but north of the Changjiang Estuary, low temperatures (< 25 ^{o}C) were recorded.

CHL concentrations were high (> 5 mg m^{-3}) along the coast and adjacent areas, but decreased sharply offshore, where low values (< 0.1 mg m^{-3}) were recorded in the Kuroshio region (Fig. 2 d - f). In 2014, a broad swath of High CHL (> 1 mg m^{-3}) extended northward into the Yellow Sea in 2012, a feature not observed in the other two years (Fig. 2 e).

Delineation of eater masses based on T-S plots

Four major water masses were defined by a temperature versus salinity (*T-S*) plot for samples from the upper 100 m in our study areas (Fig. 3.3). Previous studies, (Zhang et al. 2007; Zhou et al. 2008), have defined the CDW as low salinity (< 30) and temperature > = 23℃. These included waters from the upper layer (depth < 15m), and for stations sampled in 2011, 2013 and for one station in 2014. The KW are characterized by salinities greater than 34 and distinctive high temperature, although the shallow layers are potentially mixed with coastal water of lower salinity (Gong et al., 1996; Umezawa et al. 2014). For this study, the KW was defined by high salinity (>

32.9) and high temperature (>= 23 ^{o}C), characteristics that were observed from 0 to 65 m, including at stations that sampled in 2012 and 2014. A cold water mass with temperature < 19 ^{o}C was observed from 20-40 m during 2011 and 2013, and from 40-65 m in 2012 and 2014 and these waters were designated as Kuroshio subsurface water (KSSW). The water masses in between these three were marked as mixed waters.

From the distribution of each water mass (Fig. 3.4) and the depth of each water mass (Fig. 3.3), the surface waters west of ECS in 2011 and 2013 were classified as CDW and KSSW at depth (Fig 4 a, b); KW covered areas east of the ECS and TS and KSSW were found in the central ECS, extending northward towards the western side of TS (Fig. 3.4 b, c).

3.2.2 Vertical observations

Temperature and salinity

Strong stratification of the water column was observed in 2011, along a west to east transect, (124.6 ^{o}E to 128.8 ^{o}E; ECS-2011), (Fig. 5). A thermocline was detected at around 10-20 m in the west but at deeper layers toward the east indicating the presence of a northward flowing Kuroshio branch at eastern stations. Cold bottom water was observed at the central stations, indicated by a sharp decrease in temperature to less than 15 ^{o}C below the thermocline (Fig. 3.5 a). Salinity was greater than 33 at depths deeper than 40m, whereas, large variations (28 - 33) were observed in the upper layers specifically in the western stations strongly influenced by low salinity CDW (salinity < 30). Waters strongly characteristic of the CDW with strong stratification was observed in the upper 10m (Fig. 3.5 d).

Along transect TW-2012, low salinity water was observed in both the southern and northern stations in the upper 10 m indicating the influence of ECS water that was transported from ECS to TS along Kuroshio from 32^{o}N to 34 ^{o}N (Fig. 3.5 e). In the middle of the transect (32.5 - 33.5^{o}N), salinities were higher with values of about 32.5 in the upper layers. The core of Kuroshio water was indicated by high salinity water (33.0 -34.5) below 50 m in the south (~32.5^{o}N) and but it rose to about 30 m in the north (~33.5^{o}N) (Fig. 3.5 e). High temperature (> 25 ^{o}C) waters at southern stations extended to deeper waters up to 30 m but decreasing sharply to 16 ^{o}C at 70 m. A cold water mass was observed at much shallower depths of around 30 m at the northern stations (~34^{o}N) (Fig. 3.5 b). As a result, variations in the temperature at TS-2012 formed a deep thermocline at 50 m in the south which gradually rose to the shallower depths, around 20 m when it moved northward (Fig. 3.5 b).

In transect KW-2014, high salinity (S > 33) and high temperature (T > 25) Kuroshio waters characterized the most water column (Fig. 3.5 c). The eastern side around 128 ^{o}E was especially characterized by surface temperatures higher than 29 ^{o}C, and bottom salinities higher than 34. However, low salinity water (salinity < 30) was observed in surface waters of the eastern stations (Fig. 3.5 f).

Nutrient concentrations

Along ECS-2011, high DIN (> 15 μM) and SiO_2 (> 6 μM), but low DIP (<0.1 μM) concentrations and high N:P ratios > 50 were associated with the low salinity CDW which extended up to 10 m at the 2 westernmost stations (Fig. 3.6 a, d, g, j). DIN and DIP were depleted in the upper layers at other offshore stations, whereas high SiO_2 (> 6 μM) was measured at all stations and depths except the KW region (128.5 ^{o}N). High DIN and DIP was measured at deeper layers, forming a nitracline at about 20-80 m from the nearshore CDW stations and extending to the offshore KW stations (Fig 6. a, g). N:P ratios were generally less than those observed below the nitracline, except for high values observed at eastern stations where KSSW flowed (Fig. 3.6 j).

Both DIN and DIP were generally depleted in upper layers of transect TW-2012, with N:P ratios < 10 (Fig. 3.6 b, h). A nitracline formed around 40-50 m from south to north. Noticeably high DIN and DIP waters were found from 20-40 m with relatively higher N:P ratios (> 16) in upper layers in northern stations. SiO_2 was much lower (< 3 μM) than that were observed in the ECS-2011 (Fig. 3.6 d, e).

Transect KW-2014 showed similar low nutrient concentrations in upper layers as

TW-2012. High nutrients (DIN > 9, DIP > 0.6) were only measured in the deeper layer (> 60 m) of the one station in the east. N:P ratios were close to 16 in deep waters (depth > 50 m) of this transect (Fig. 3.6 c, f, i, l).

Phytoplankton communities

Vertical profiles recorded to 80 m, revealed the existence of a Sub-surface Chlorophyll Maxima (SCM) at all stations along ECS-2011 and TS-2012 (Fig. 3.7 a, b). In ECS-2011, the depth of SCM was only around 14 m (CHL = 6.75 mg m^{-3}) at western stations but deeper observed around 65 m (CHL = 1.03 mg m^{-3}) at the eastern station (Fig. 3.7 a). A double SCM (CHL= 3.22 mg m^{-3} at 25 m; CHL= 3 mg m^{-3} at 50 m) was observed at station 127 ^{o}E. Brown algae accounted for 60% of the CHL in SCM (Fig. 3.7 d), cyanobacteria also dominant the upper layers above the SCM (40% - 80%) (Fig. 3.7 g) and, green algae and cryptophytes composed up to 20% - 40% of the CHL below the SCM (Fig. 3.7 j, m). Generally, surface and deep waters of coastal waters had distinct phytoplankton groups, whereas at offshore stations, cyanobacteria and brown algae dominated, especially at stations along 126.5 ^{o}N.

In TW-2012, SCMs were deeper around 40-50 m from south (32.75 ^{o}N) to north (Fig. 3.7 b). CHL concentrations in the SCMs varied between 1.64 and 8.42 mg m^{-3}, and the highest value was observed at the northern station around Tsushima Island (34.7 ^{o}N).

Relatively shallower SCMs were observed in the central stations at 34.1- 34.7 ^{o}N. Brown algae dominated the water column except just above the SCM where cyanobacteria predominated (> 30%) (Fig. 3.7 e, h). Above the SCM, the large (> 40%) cyanobacterial populations were also found in the subsurface depth at around 20m (Fig. 3.7 h). Green algae contributed 20% to the surface CHL but were lower at deeper depths. Cryptophytes showed low abundance for the area (Fig. 3.7 k, n).

In KW-2014, waters deeper than 50 m showed relatively higher CHL (0.50 – 1.66 mg m^{-3}) than upper waters (< 0.40 mg m^{-3}) (Fig. 3.7 c). Brown algae were dominant (up to 85%) in deeper high nutrient waters to the west but were gradually replaced by green algae at eastern stations (Fig. 3.7 f, l). Cyanobacteria dominated surface waters comprising more than 60% of the low CHL waters (Fig. 3.7 f, i). Cryptophytes were observed at around 20 - 50 m from west to east of this section (Fig. 3.7 o). A comparison between vertical profiles of phytoplankton groups derived from HPLC-CHEMTAX and Multi-Exciter derived are shown in Fig. 3.9. The results from the two methods were generally consistent i.e. brown algae and cyanobacteria showed high values in deep and surface layer, respectively; green algae showed a high value in the deep layer of the eastern station in 128 ^{o}E (Fig.9 right). In addition, the high-resolution fluorescence profiles provided greater detail of the distribution patters of phytoplankton groups than is possible by HPLC-CHEMTAX pigment analysis alone.

3.4 Discussion

3.4.1 Vertical observations in the ECS and TS

This study focused on the vertical structure and variability of water masses and their influence on phytoplankton communities in the ECS and TS. Surface ocean color CHL images for the four summers that comprised our study, revealed high CHL near Changjiang Estuary, gradually decreasing offshore (Fig. 2). These spatial distribution patterns are highly consistent with previous studies (Yamaguchi et al., 2012, 2013). However, what our study reveals is that besides surface variations, there are large changes in temperature and CHL with depth which needed to be examined, in order to understand how the movement of water masses in deeper layers can affect phytoplankton composition (Furuya et al., 2003, Liu et al., 2012).

The eastern ECS generally maintains its characteristics of oceanic waters, the KW flows into the ECS forming a mixture of water masses with CDW and water from the Yellow Sea, flowing further into the TS as TW (Isobe et al., 2002). In the ECS, high temperature, low salinity and high N:P ratios were observed above 20 m indicating the influence of CDW. SCMs were located in the upper waters < 30 m (Fig. 3.8 a - g). The Phytoplankton groups varied annually: brown algae dominated in 2013, while mixed phytoplankton communities were recorded in 2011. CDW flowing into the mid-shelf of the ECS, caused DIP-limitation and strongly inhibited the growth of large phytoplankton such as diatoms and dinoflagellate (denoted as brown algae in this study) (Wang et al., 2014, Xu et al., 2018, Wang et al., 2016, Ishizaka et al., 2021, Gomes et al., 2018). Similar patterns were reported for surface CDW dominated waters by Xu et al. (2018) who suggested dominance by brown algae in 2013 was likely caused by the offshore movement of low N:P-ratio CDW to the mid-shelf ECS. At locations where vertical mixing was strong enough to erode the halocline, high salinity and high nutrient water that shoaled into the euphotic zone supported phytoplankton growth to form SCMs near the nitracline (Lee et al., 2017).

In TS (2012) and Kuroshio region (2014), surface CHL was low and SCMs were recorded below 30 m (Fig. 3.8 c). Brown algae contributed to the high CHL in the entire euphotic column especially in SCM (Fig. 3.8 i). A previous study in TS showed that 70% of the freshwater at upper depths (< 50 m) flowed from the ECS to TS, however, DIN and DIP had been depleted by the phytoplankton in the ECS (Isobe, et al., 2002, Morimoto et al., 2009). Therefore, the dominance of brown algae represents a typical feature of phytoplankton composition in coastal regions of global oceans (Simpson and Sharples 2012, Wang et al., 2014, Wang et al., 2018). In the Kuroshio region (2014), brown algae were replaced by green algae in the SCMs at deeper depths. The paucity of nutrients in the surface waters of the Kuroshio region greatly limited the growth of large phytoplankton, but conversely facilitated growth of small phytoplankton because of their high photosynthetic efficiency under stable light conditions (Ishizaka et al., 1994, Wang et al., 2014).

3.4.2 Application of multiple excitation fluorometer on the study of phytoplankton community structure

Phytoplankton groups derived using multiple excitation fluorometer and calibrated with similar phytoplankton community distribution derived using in-situ HPLC pigment biomarkers, offers two major advantages. Firstly, this submersible profiling instrument was able to provide accurate high-resolution vertical profiles of phytoplankton in ECS and TS far greater than that possible by discrete depth HPLC-pigment samples (Fig. 3.9 left). At almost all stations HPLC pigment analysis could not adequately capture the phytoplankton variability associated with different water masses. For example temperature, nutrient and CHL concentrations all showed clear vertical and spatial changes (Fig. 3.5 c; Fig. 3.6 c, f, i, l; Fig. 3.7 c) but it was difficult the associated fine-scale changes in phytoplankton composition with HPLC derived phytoplankton groups (Fig. 3.9 left). Conversely the fluorometer provided phytoplankton abundance every 1 m (Fig. 3.9 right) with generally results that were consistent with HPLC derived phytoplankton groups.

The large amount of data generated make it possible to observe the interaction between water mass changes and phytoplankton variabilities on a larger scale. Three transects were chosen to show the relative abundances of phytoplankton groups in Kuroshio water (KW-2014), Tsushima Strait (TW-2012) and ESC (ECS-2011). Even in KW-2014 which was mostly affected by Kuroshio water, temperature and nutrient gradients resulted in three-layers of different phytoplankton groups. Surface and deep water were gradually mixed at 20-50 m, with temperatures of 22-24.5 ℃, and nutrient concentrations were low. Consequently, CHL in the surface waters was low, and cyanobacteria and green were the major contributors to CHL. Below 50 m, at the western and eastern stations, brown and green algae contributed to the higher CHL. Compared to KW-2014, section TW-2012 was mostly dominated by brown algae, but the shift to dominance by green algae (probably prochlorophytes, as discussed in the following paragraph) at the eastern station is probably related to the flow of low-nutrient, high-temperature Kuroshio water (Liu et al., 2016, Ishizaka et al., 2021). This was well captured by the fluorometer making possible large-scale observations, especially for retracing imperceptible variations, difficult to observe by sampling at discrete depths.

The objective of the Multi-Exciter calibration in our study is to extract spectral characteristics of different phytoplankton groups from *in-situ* HPLC CHEMTAX data.

Compared to the initial calibration, the *in situ* calibration in this study takes advantage to obtain spectral differences of each phytoplankton group without defining “norm spectra”. The “norm spectra” for the Multi-Exciter, was initially calibrated by the manufacturing company with freshwater species cultured in the laboratory (Yoshida et al., 2011), similar to another multiple excitation fluorometer, the FluoroProbe. Several researchers who used the FluoroProbe pointed out that the accuracy of the fluorometer is largely dependent on the calibration (See et al 2005; Richardson et al 2010), and the determination of the norm spectra of each group is the fundamental component for evaluation (Beutler et al., 2002). It has been known that the norm spectra between species are not always the same under different environmental conditions and varied phytoplankton composition (Loftus and Seliger 1975), which leads to under/over estimation by the fluorometer (Beutler et al., 2002; Alexander et al 2012). Therefore, applying the present model make it possible to use the Multi-Exciter without measuring cultured algae spectra from the specific study areas.

There are however some limitations to the use of multiple excitation fluorometers in the field. Firstly, the florescent spectra data in shallow layers (less than 5m in this study) was influenced by non-photochemical quenching under high light conditions, so that it cannot correctly reflect phytoplankton physiological properties and total abundance and species composition may able be influenced. (Koblížek et al 2001, Morrison et al 2003).

Secondly, our approach cannot resolve as many phytoplankton groups as HPLC derived pigments in association with CHEMTAX. For example, in this study, prochlorophytes were not included for calibration, whereas this group was frequently observed in the Kuroshio region of the ECS (Furuya et al., 2003, Xu et al., 2018). Prochlorophytes which are part of cyanobacterial group, are about 0.6 - 0.8μm in size and contain the dominant and characteristic pigment divinyl-chlorophyll a. The spectral shape of divinyl-chlorophyll a is similar to CHL, showing fluorescence emission in the red band which overlaps with that of CHL (Zapata et al., 2000, Bricaud et al., 2004). The complementary pigments of prochlorophytes include chlorophyll b_2, zeaxanthin and α-carotene, which is a similar pigment composition to prasinoxanthin containing prasinophytes (Goericke & Repeta 1992). The Multi-Exciter will detect this group as green algae, rather than cyanobacteria. Our HPLC analysis of pigments shows that divinyl-chlorophyll *a* was present in the Kuroshio region (0.01~0.35 mg m^{-3}), with maximum values in the SCM of KW-2014. The Multi-Exciter detected green algae in association with the high KW in mixed layers where temperature was around 22 to 24.5 °C (Fig. 3.5 c, Fig.7 I). Therefore, the green algae detected by the Multi-Exciter in the KW region of 2014 should be revised as prochlorophytes, as previous studies have revealed that prochlorophytes were temperature sensitive and restricted in Kuroshio water in the eastern ECS (Lee et al 2014, Ishizaka et al., 2021). This example serves to stress the necessity and importance of using a combination of Multi-Exciter and HPLC pigment analysis at certain depths to ascertain the whole structure of phytoplankton groups.

3.5 Conclusions

In this study, we used a newly developed multiple excitation fluorometer to estimate the vertical distribution of phytoplankton groups in the ECS and TS. Compared to the historical approach of pigment biomarkers derived using HPLC separation of phytoplankton pigments, the in-situ fluorometer provided a very large dataset, of high-resolution, vertical profiles of phytoplankton groups, which allowed us to infer their relationship with different water masses. Cyanobacteria were highly associated with low-CHL KW both spatially and vertically. Brown algae dominated the TW showing the features of the coastal waters. Green algae and cryptophytes were regionally distributed: cryptophytes contributed to the deeper layers of SCM in CDW and KW possibly influenced by nutrient and light conditions, and prochlorophytes were found in association with the high-temperature KW. Overall, the newly developed in-situ multiple excitation fluorometer successfully detected phytoplankton groups in both coastal and oceanic waters and provided high-resolution profile data making observations of large-scale variations in phytoplankton groups in association with dynamic water masses an exciting possibility.

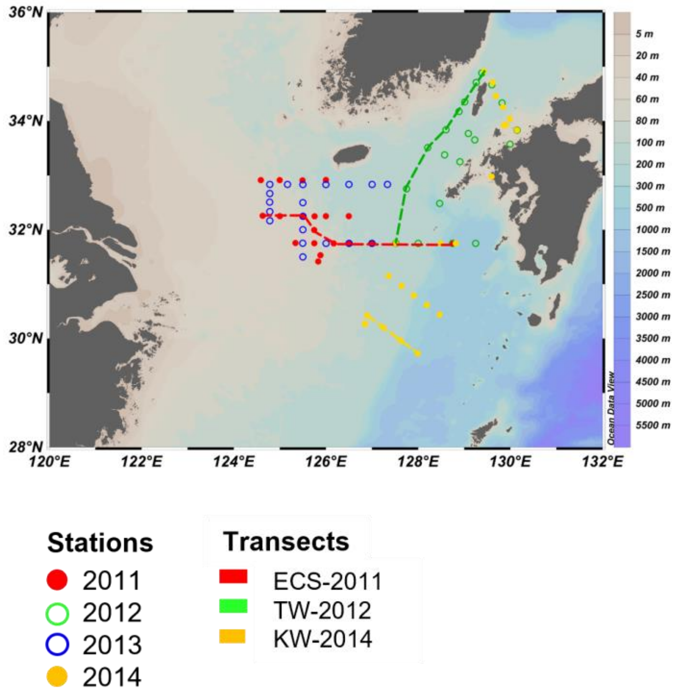

Fig. 3.1. Sampling locations for the four cruises in the East China Sea (ECS) and Tsushima Strait in late July of 2011 - 2014. Three transects (dashed line) in East China Sea (ECS-2011), Tsushima Water (TW-2012) and Kuroshio Water (KW-2014) were selected to compare vertical profiles of water properties and phytoplankton distributions.

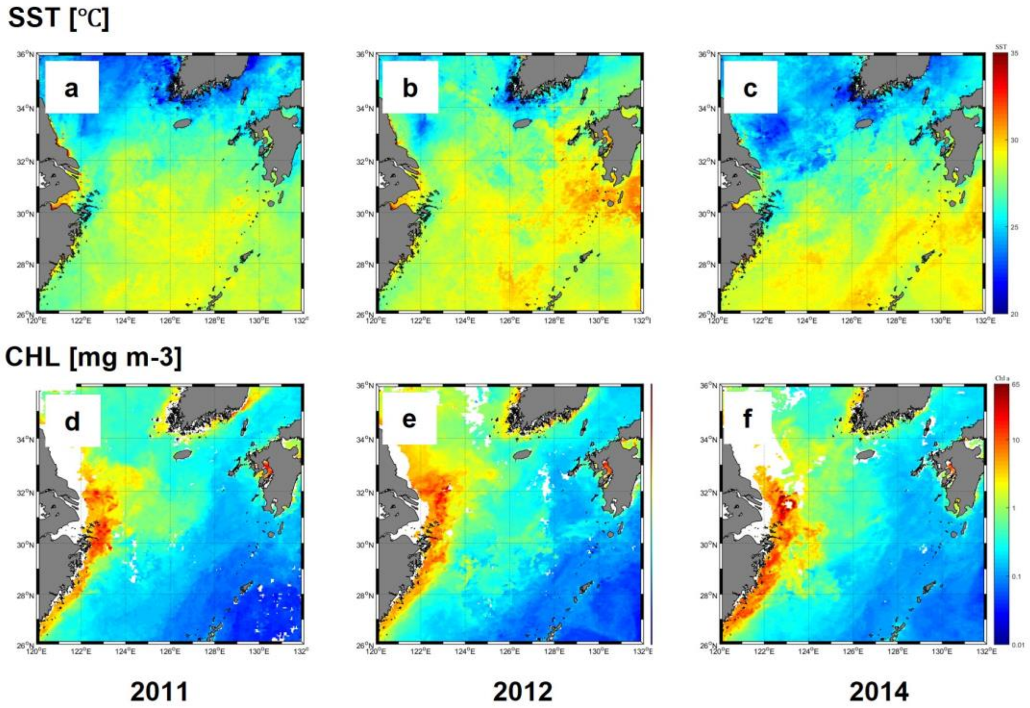

Fig. 3.2. Monthly composites of SST (℃) and CHL (mg m^{-3}) in the ESC and TS during 2011-2014 in July.

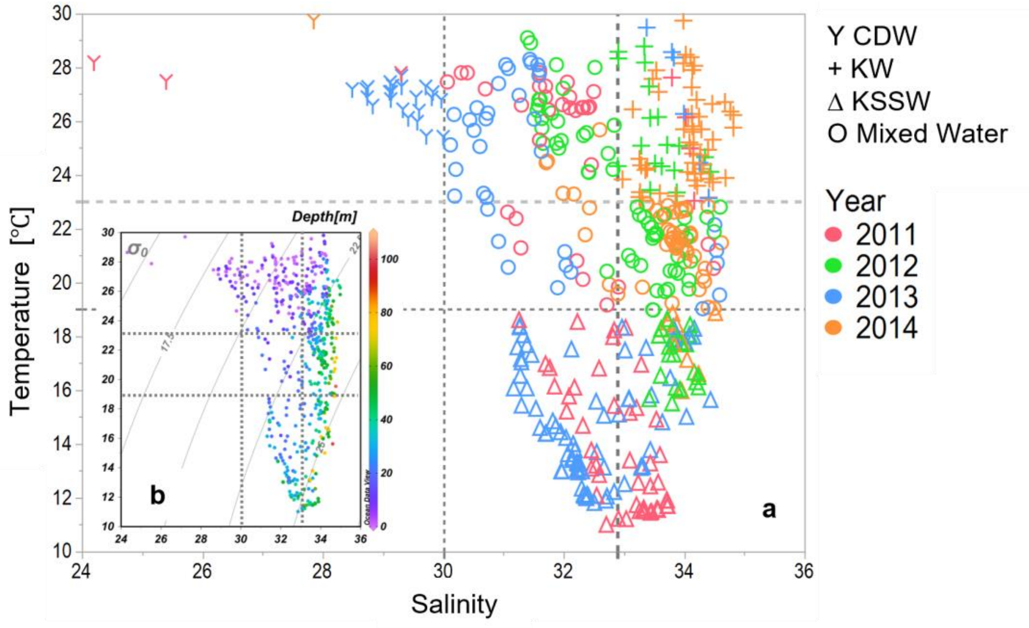

Fig. 3.3. (a) Temperature-salinity (*T-S*) plot of the upper 100 m depth delineating water masses. CDW (Y) were defined as T > 23℃, S < 30, KW (+) were defined as T > 23 ℃, S >= 32.9, KSSW (Δ) were defined as T <19 ℃, and the rest data were defined as Mixed Water (O). (b) Depth of the samples of the *T-S* plot.

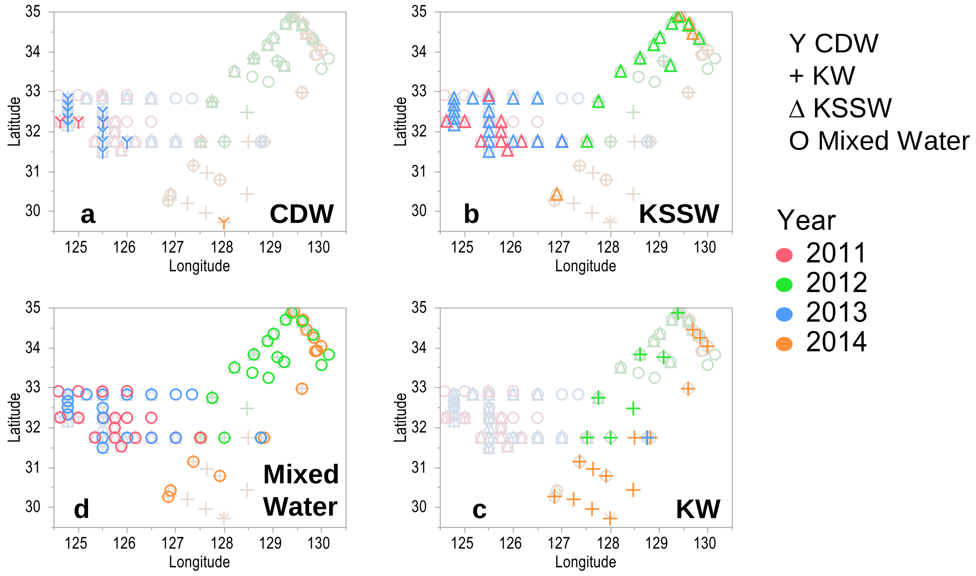

Fig. 3.4. Distribution of each water mass that defined in Fig. 3.3 in the study areas.

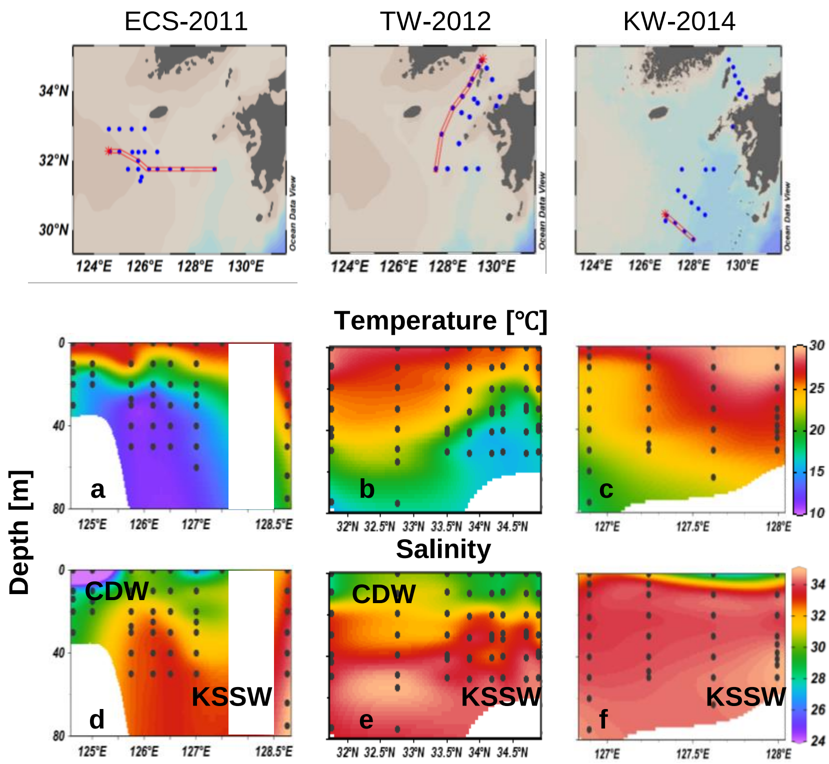

Fig. 3.5. Vertical distributions of temperature (℃) (a-c), salinity (d-f) in the tree selected transects .Black dots are sampling data.

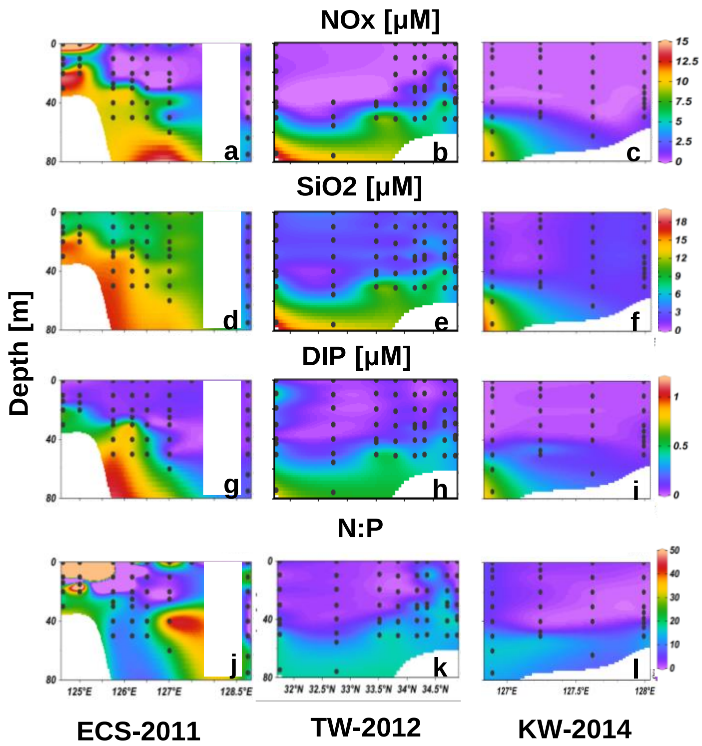

Fig. 3.6. Vertical distributions of NOx (a - c), SiO_2 (d - f), DIP (g - i) (μM) and N:P (j - l) in the tree selected transects. Black dots are sampling data.

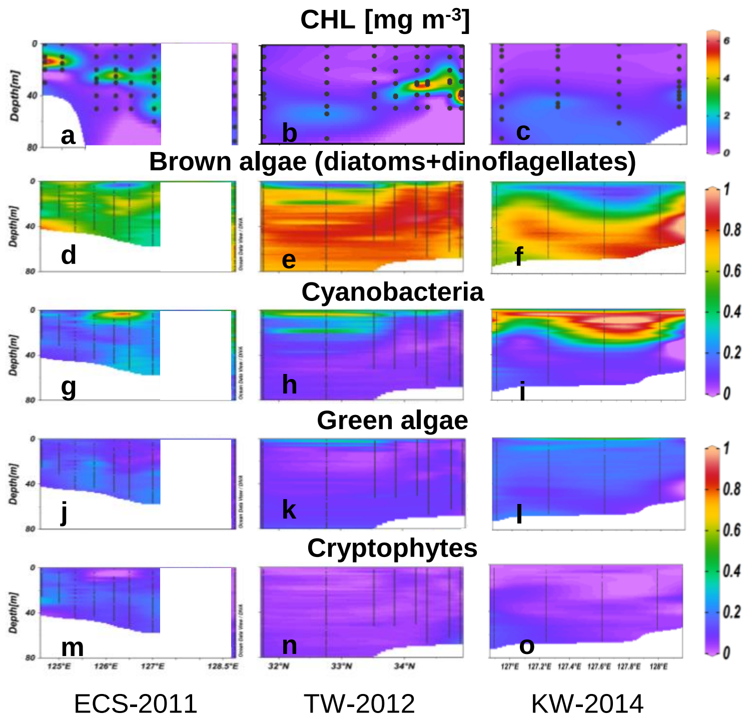

Fig. 3.7. CHL concentrations (a - c) (mg m-3) and the relative abundance of phytoplankton groups (g - o) estimated by Multi-Exciter in the three selected transects. Black dots are sampling data.

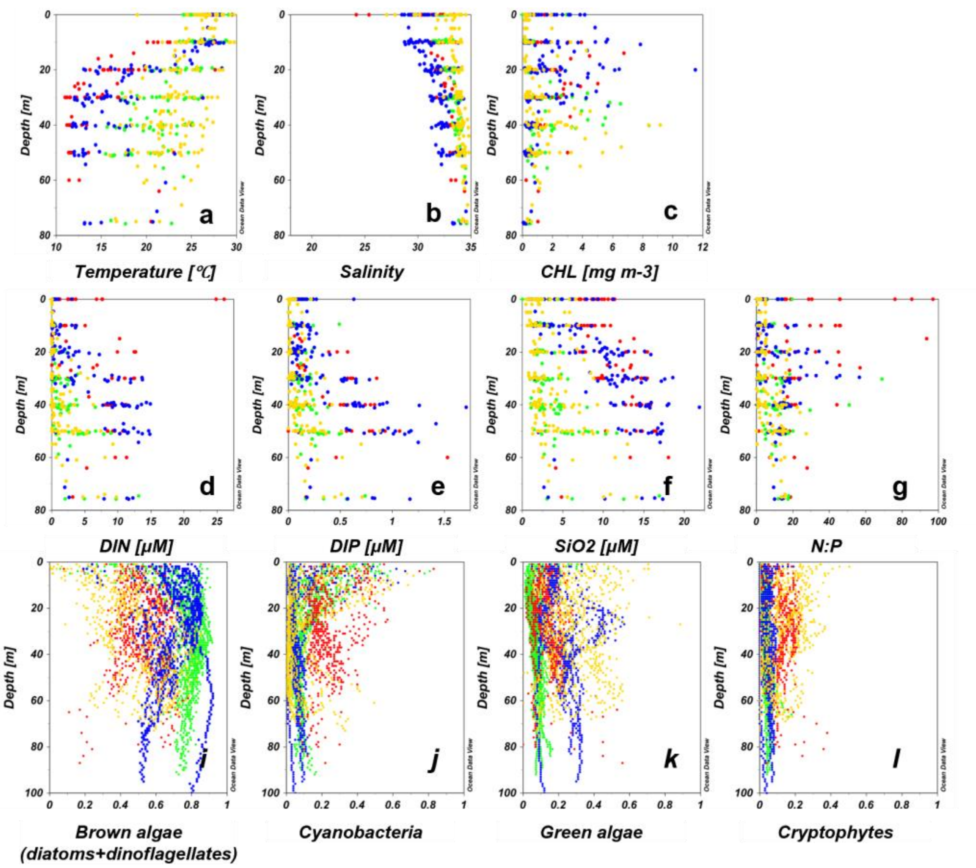

Fig. 3.8. Vertical profiles of environmental factors (a - h) and Multi-Exciter-derived phytoplankton groups during the four courses i - j, 2011: red, 2012: green, 2013: blue, 2014: yellow) (i - l) for each water.

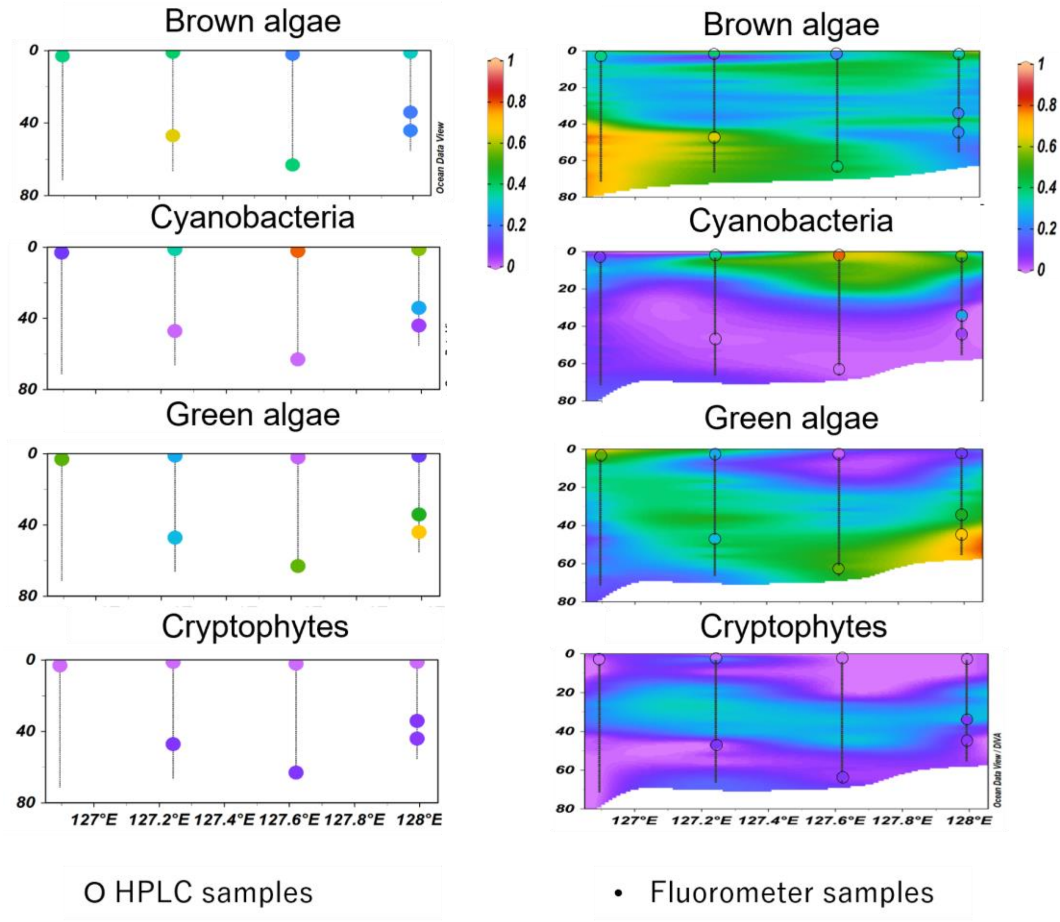

Fig. 3.9. Comparison between HPLC-CHEMTAX (left) and the Multi-Exciter (right) derived vertical profiles of phytoplankton compositions. The colored dots were samples measured by the HPLC method; these samples overlayed on the profiles presented by the fluorometer and marked with black circles.

Chapter4 General Discussion

In Chapter 2, inter-annual variations in CHL were clear in the west of the study area and indistinctive eastward in accordance with variations in temperature, salinity and nutrients brought about by mixing of the KSW, CDW and SW (Fig.2.3). This distribution is consistent with previous studies (Yamaguchi et al. 2012; 2013) which also showed that CHL concentrations were higher in coastal waters and lower offshore. Interestingly, the high CHL (> 1 mg m^{-3}) during the high-DIP-years of 2009/2013 was mainly contributed by diatoms and dinoflagellates, while during high-NOx-years of 2010/2011 it showed mixed populations of cyanobacteria, chlorophytes, prymnesiophytes and a small component of diatoms. Changjiang river discharge were only observed in higher volume in 2010 during the four periods (Fig. S1), whereas, nutrient concentration in the CDW showed clear variation between 2010/2011 and 2009/2013. Nutrient variations across the continental shelf of the ECS shows nonconservative mixing behavior, DIN concentrations were already modified before or during their transport over the salinity front (=31) and some nutrients, particularly DIP were depleted before it was transported the northeastern ECS in summer (Gao et al., 2015). Therefore, the major factor controlling inter-annual variations of CHL in the ECS in summer was suggested to be the extent of DIP-limitation of the CDW during its eastward advection to offshore.

In 2010/2011, DIP-limitation was indicated by high ExcN in the fresher CDW which created strong stratification around 124.5 ^oE in our study area. Such low salinity water and consequent stratification are comparable to the conditions observed further west near the Changjiang Estuary around 122 ^oE to 124 ^oE in summer (Chen et al. 2008, Tseng et al. 2014, Guo et al. 2014, Jiang et al. 2015), suggesting that CDW was less diluted by seawater during its extension into our study area in 2010/2011 (Fig. 2.3f, g). Correspondingly, DIP concentrations in the CDW were generally < 0.2 μM, while NOx were in excess (ExcN > 0) and this led to extremely high N:P ratios (> 100) (Fig. 2.3r, s). These results indicate that the fresher CDW could induce DIP limitation further east in the ECS in 2010/2011.

In 2009/2013, CDW showed high DIP and ExcN < 0. Such waters were assembled in Cluster 2 which showed high DIP and relatively high salinities and low temperatures. PCA analysis also showed a negative correlation between temperature and DIP. It is well known that CDW are deficient in DIP (Chen and Wang 1999; Wang et al. 2003; Chen et al. 2008), therefore high DIP in 2009/2013 in the CDW probably resulted from the mixing of CDW with subsurface nutrient-rich waters.

Upwelling of nutrient rich KIW along the shelf slope has been suggested as a primary source of high DIP onto the ECS shelf (Ito et al. 1994; Chen et al. 1996). A branch of the KIW from the southwest of Kyushu crosses the ECS shelf (Ito et al. 1994;

Guo et al. 2006). In this study, interannual variations in phytoplankton community in response to varying N:P ratios in the CDW (Fig. 2.13). If the CDW is highly stratified (salinity < 28 in our study) suppressing near surface water mixing with subsurface water, then surface DIP is rapidly consumed by phytoplankton in the outer Changjiang Estuary. This results in DIP-limitation and the dominance of smaller phytoplankton, such as cyanobacteria as observed in 2010/2011 during our study (Fig. 2.13a). On the other hand, when intensive coastal upwelling occurs, it brings high-DIP subsurface water upward which mixes with the surface CDW around Changjiang estuary. The resulting CDW with low N:P ratio advected eastward, and sustained the growth of larger phytoplankton, such as diatoms and dinoflagellates, in offshore waters (Fig. 2.13b) as observed in 2009/2013 during our study.

The application of *in-situ* submersible instrument Multi-Exciter in Chapter 3, provided high-resolution profiles to improved our understanding on phytoplankton community in vertical layers, especially for adjacent areas of Changjiang Estuary in summer.

Three transects were chosen to show the relative abundances of phytoplankton community in Kuroshio water (KW-2014), Tsushima Strait (TW-2012) and ESC (ECS-2011). Minimal CHL (< 1 mg m^{-3}) appeared in the upper layers of KW-2014 (Fig. 3.7 c), where was associated with KW with a domination of cyanobacteria (> 50%)

from surface until 30 m at depth (Fig. 3.7 i). SCM (CHL maxima = 7.85 mg m^{-3}) composed by the mixture phytoplankton groups in different layers were found in ECS-2011 (Fig.3.7 a, d, g, j, m) where influenced by CDW and KSSW in the upper and deeper layers, respectively (Fig. 3.4 a, b). Cyanobacteria and brown algae dominated in the upper and deeper layers respectively in TW-2012 (Fig. 3.7 e, h) where influenced by KW and KSSW in the upper and deeper layers. If we compare these finding to samples like HPLC which can only derived from certain depths, multiple excitation fluorometer provided data in every meter which was sufficient to show continuous vertical profiles covered the whole region of ECS. Apparently, the performance of Multi-Exciter have greatly enhanced the sufficiency and possibility to apply *in-situ* data sampling to large scale observations, especially for retrace the imperceptible variations which were difficult to be observed by stratified sampling at limited layers.

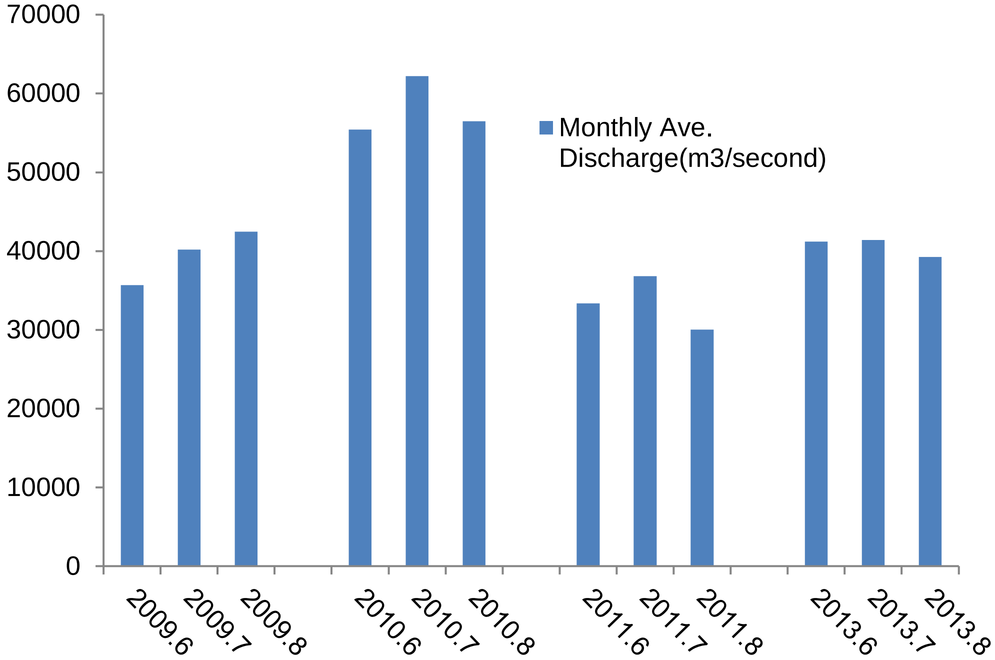

Fig 4. S2. Monthly averaged Changjiang river discharge at Datong station. Data source:

http://www.mwr.gov.cn/sj/tjgb/szygb/

Chapter5 General Conclusions

5.1 Concluding remarks

Our study is the first to document inter-annual variations in the phytoplankton community of the mid-shelf ECS in relation to the nutrient stoichiometry resulting from variations in the water masses of the ECS. Compared to the low nutrient concentrations and invariant N:P ratios that typified the Kuroshio waters, significant differences in water properties and nutrient concentrations were observed in the CDW influenced region during the four summers of sampling. DIP concentrations in the CDW were low in 2010/2011, but it was remained in 2009/2013. As a result, mixed populations of phytoplankton were observed in 2010/2011 while diatom domination was observed in 2009/2013. This study shows that DIP supply is crucial in determining the phytoplankton composition in the mid-shelf ECS. Compared to the highly stratified CDW in 2010/2011, CDW in 2009/2013 was in all probability already mixed with the upwelled subsurface waters from the coastal region supporting a more eastward dispersal of high phytoplankton concentrations into the mid-shelf ECS over longer time periods.

Compared to historical approach, the newly calculated *in-situ* fluorometer provided vast high-resolutions vertical profiles of phytoplankton groups, which filled the gap on vertical distributions of phytoplankton communities in the three distinguished water masses. In CDW, certain concentration of green algae and cryptophytes were observed below SCM layers, where were higher in NOx, SiO2 and DIP. It is comparable to coastal water of TW which was composed by brown algae (diatoms and dinoflagellates) in the whole water column, in consistent with N:P ratio around 10 to 20 below SCM. In KW, high concentration of cyanobacteria were observed to be extended to deeper layer around 30 m in associated with low nutrients and low CHL.

5.2 Suggestions for future researches

As DIP in the CDW were fast consumed by phytoplankton communities in the Changjiang Estuary, the offshore region of the ECS has a well-known fact of DIP-limitation which affects the growth of large phytoplankton. The only possibility source of DIP was considered from waters in deep layer. Episodic events like typhoons may cause localized upwelling on the ECS shelf and consequently some nutrient enhancement (Siswanto et al. 2008). However, the *T-S* plot and nutrient profiles for our study area did not show any indication of localized upwelling or vertical mixing, or were any typhoon events recorded in July of the years that we sampled. KIW upwelling along the shelf slope has been suggested as a primary source of high DIP into the ECS shelf (Ito et al. 1994; Chen et al. 1996). In this study, intensive nearshore wind driven coastal upwelling were observed, which probably brought DIP-rich water upward and mixed with the surface CDW around Changjiang estuary. Coastal upwelling in 2009 and 2013 was indicated by sea surface temperature (SST) anomalies and a northward wind pattern along the coast of China (Fig. 2.S1). However, surface data were not given directly explanation on mechanism of nutrient transportation from deep layers. Future study on vertical mixing in respect of physical water movements are necessary to shed light on the inter-annual variations in the interaction of Changjiang river plume and coastal upwelling both of which drive nutrient inputs into the ECS shelf region, and consequently determine the phytoplankton community structure and the overall biogeochemical cycling within the ECS.

References

Armstrong FAJ, Stearns CR, Stickland JDH (1967) The measurement of upwelling and subsequent biological processes by means of the TechniconTM AutoanalyzerTM and associated equipment. Deep Sea Res 14:381–389.

Beutler, M., Wiltshire, K. H., Meyer, B., Moldaenke, C., Lüring, C., Meyerhöfer, M., Hanse, U.-P. & Dau, H. (2002) A fluorometric method for the differentiation of algal populations in vivo and in situ. Photosynthesis Research, 72(1): 39-53.

Brewin R, Sathyendranath S, Hirata T, et al (2010) A three-component model of phytoplankton size class for the Atlantic Ocean. Ecol Model 221:1472–1483.

Bricaud, A., Claustre, H., Ras, J., & Oubelkheir, K. (2004). Natural variability of phytoplanktonic absorption in oceanic waters: Influence of the size structure of algal populations. Journal of Geophysical Research: Oceans, 109(C11).

Chen C, Wang S (1999) Carbon, alkalinity and nutrient budgets on the East China Sea continental shelf. J Geophys Res Oceans 1978 2012 104:20675–20686

Chen CTA (1996) The Kuroshio intermediate water is the major source of nutrients on the East China Sea continental shelf. Oceanologica Acta, 19(5), 523-527

Chen CTA (2008) Distributions of nutrients in the East China Sea and the South China Sea connection. J Oceanogr 64:737–751. doi: 10.1007/s10872-008-0062-9.

Chen CTA (2009) Chemical and physical fronts in the Bohai, Yellow and East China seas. Journal of Marine Systems, 78(3), 394-410.

Chen YL, Chen HY, Gong GC, et al (2004) Phytoplankton production during a summer coastal upwelling in the East China Sea. Cont Shelf Res 24, 1321–1338

Dorado S, Booe T, Steichen J, et al (2015) Towards an Understanding of the Interactions between Freshwater Inflows and Phytoplankton Communities in a Subtropical Estuary in the Gulf of Mexico. Plos One 10:e0130931

Fang TH (2004) Phosphorus speciation and budget of the East China Sea. Cont Shelf Res, 24(12), 1285-1299.

Finkel ZV (2007) Does phytoplankton cell size matter? The evolution ofmodern marine food webs. In: Evolution of aquatic photoautotrophs (eds.Falkowski, PG & Knoll, AH). Academic Press, San Diego, pp. 333–350.

Fujiwara A, Hirawake T, Suzuki K, et al (2014) Timing of sea ice retreat can alter phytoplankton community structure in the western Arctic Ocean. Biogeosciences 11:1705–1716.

Furuya K, Hayashi M, Yabushita Y (2003) Phytoplankton dynamics in the East China Sea in spring and summer as revealed by HPLC-derived pigment signatures. Deep-Sea Res. II, 50, 367–387.

Gao L, Li D, Ishizaka J, Zhang Y, Zong H, & Guo L (2015). Nutrient dynamics across the river-sea interface in the C hangjiang (Y angtze R iver) estuary—E ast C hina S ea region. Limnology and Oceanography, 60(6), 2207-2221.Gettings R, Townsend D, Thomas M, Karp-Boss L (2014) Dynamics of late spring and summer phytoplankton communities on Georges Bank, with emphasis on diatoms, Alexandrium spp., and other dinoflagellates. Deep Sea Res Part Ii Top Stud Oceanogr 103:120–138.

Goericke R, Repeta DG (1992) The pigments of Prochlorococcus marinus: the presence of divinyl chlorophyll a and b in a marine procaryote. Limnol Oceanogr 37:425-433

Goes JI, Gomes HDR, and Chekalyuk AM, et al (2014) Influence of the Amazon River discharge on the biogeography of phytoplankton communities in the western tropical North Atlantic, Prog. Oceanogr., 120, 29–40, doi:10.1016/j.pocean.2013.07.010.

Gomes H R, Xu Q, Ishizaka J et al (2018) THE INFLUENCE OF RIVERINE NUTRIENTS IN NICHE PARTITIONING OF PHYTOPLANKTON COMMUNITIES–A CONTRAST BETWEEN THE AMAZON RIVER PLUME AND THE CHANGJIANG (YANGTZE) RIVER DILUTED WATER OF THE EAST CHINA SEA. Frontiers in Marine Science, 5, 343.

Gong GC, Chen YL, Liu KK (1996) Chemical hydrography and chlorophyll a distribution in the East China Sea in summer: implications in nutrient dynamics. Cont Shelf Res 16:1561–1590.

Gong GC, Wen Y. HB. Wang W and Liu GJ (2003) Seasonal chlorophyll a concentration, primary production and environment conditions in the subtropical East China Sea. Deep-Sea Res. II, 50, 1219–1236.

Guo S, Feng Y, Wang L, et al (2014) Seasonal variation in the phytoplankton community of a continental-shelf sea: the East China Sea. Mar Ecol Prog Ser 516:103–126.

Guo X, Miyazawa Y (2006) The Kuroshio onshore intrusion along the shelf break of the East China Sea: the origin of the Tsushima Warm Current. J. Phys. Oceanogr., 36, 2205–2231.

Hecky RE, Kilham P (1988) Nutrient limitation of phytoplankton in freshwater and marine environments: A review of recent evidence on the effects of enrichment, Limnology and Oceanography, 33..

Heukelem LV, and Thomas CS (2001) Computer-assisted high-performance liquid chromatography method development with applications to the isolation and analysis of phytoplankton pigments, J. Chromatogr. A, 910, 31–49. s.

Hirata T, Hardman-Mountford N, Brewin R, et al (2011) Synoptic relationships between surface Chlorophyll-a and diagnostic pigments specific to phytoplankton functional types. Biogeosciences 8:311–327.

Ishizaka J, Kiyosawa H, Ishida K, et al (1994) Meridional distribution and carbon biomass of autotrophic picoplankton in the Central North Pacific Ocean during Late Northern Summer 1990. Deep-Sea Res. Part I: Oceanographic Research Papers, 41(11-12), 1745-1766.

Ishizaka, J. (2021). 3.2 Phytoplankton, in Oceanography of the Yellow Sea and East China Sea. PICES Sci. Rep. No. 62. Eds J. Ishizaka et al., North Pacific Marine Science Organization, Sidney, BC, Canada, 224-243.

Isobe A (1999) On the origin of the Tsushima Warm Current and its seasonality. Cont Shelf Res, 19(1), 117-133.

Isobe A., Ando M., Watanabe T., Senjyu T., Sugihara S., & Manda A. (2002). Freshwater and temperature transports through the Tsushima‐Korea Straits. Journal of Geophysical Research: Oceans, 107(C7), 2-1.

Ito T, Kaneko A, Tsubota H, Gohda N (1994) The characteristic distribution of silica over the East China Sea shelf slope. J Oceanogr 50:465–477.

Jeffrey SW, Mantoura RFC, Wright SW (1997) Phytoplankton pigments in oceanography:guidelines to modern methods, vol 10. Monographs on oceanographic methodology. UNESCO Publishing, Paris

Jiang Z, Chen J, Zhou F, et al (2015) Controlling factors of summer phytoplankton community in the Changjiang (Yangtze River) Estuary and adjacent East China Sea shelf. Cont Shelf Res 101:71–84.

Jiang Z, Liu J, Chen J, et al (2014) Responses of summer phytoplankton community to drastic environmental changes in the Changjiang (Yangtze River) estuary during the past 50 years. Water Research 54:1–11.

Jiao N, Yang Y, et al (2005) Dynamics of autotrophic picoplankton and heterotrophic bacteria in the East China Sea. Cont. Shelf Res., 25, 1265–1279.

Koroleff F (1983) Determination of silicon. In: Glasshoff K, Ehrhardt M, Kremling K (eds) Methods of seawater analysis, 2nd edn. Verlag Chemie, Weinheim, pp 174–183.

Lalli C, Parsons TR (1997) Biological oceanography: an introduction. Butterworth-Heinemann, pp 112-117.

Latasa (2007) Improving estimations of phytoplankton class abundances using CHEMTAX. Marine Ecology Progress Series 13–21.

Lee Y, Choi JK, Youn S, and Roh S (2014) Influence of the physical forcing of different water masses on the spatial and temporal distributions of picophytoplankton in the northern East China Sea. Cont. Shelf Res., 88 , 216-227.

Lee J Y, Kang D J, Kim I N, Rho T, Lee T, Kang C K, & Kim K R (2009) Spatial and temporal variability in the pelagic ecosystem of the East Sea (Sea of Japan): a review. Journal of Marine Systems, 78(2), 288-300.

Lee K, Matsuno T, Endoh T, Ishizaka J, Zhu Y, Takeda S, & Sukigara C (2016) A role of vertical mixing on nutrient supply into the subsurface chlorophyll maximum in the shelf region of the East China Sea. Cont. Shelf Res., 143, 139-150.

Li DW, Chen JF, Wang K, et al (2016) Contribution of Outer-Shelf Deep Water to the Nutrient Inventories in the Euphotic Zone of the Changjiang River Plume during Summer. Journal of Coastal Research, 32(5), 1081-1091.

Li J, Glibert PM, Zhou M, et al (2009) Relationships between nitrogen and phosphorus forms and ratios and the development of dinoflagellate blooms in the East China Sea. Mar. Ecol. Prog. Ser., 383: 11–26.

Lie HJ, Cho CH (1994) On the origin of the Tsushima Warm Current. Journal of Geophysical Research: Oceans.

Lin YC, Chung CC, Gong GC and Chiang KP (2014) Diversity and abundance of haptophytes in the East China Sea. Aquatic Microbial Ecology, 72(3), 227-240.

Liu HC, Shih CY, Gong GC et al (2013) Discrimination between the influences of river discharge and coastal upwelling on summer microphytoplankton phosphorus stress in the East China Sea, Cont. Shelf Res., 60, 104–112, 2013.

Liu X, Huang B, Huang Q, et al (2015) Seasonal phytoplankton response to physical processes in the southern Yellow Sea. J Sea Res 95:45–55.

Liu X, Xiao W, Landry M, et al (2016) Responses of Phytoplankton Communities to Environmental Variability in the East China Sea. Ecosystems 19:832–849.

Loftus M E, & Seliger H H (1975) Some limitations of the in vivo fluorescence technique. Chesapeake Science, 16(2), 79-92.

Liu X, Huang B, Liu Z, Wang L, Wei H, Li C, & Huang Q (2012) High-resolution phytoplankton diel variations in the summer stratified central Yellow Sea. Journal of oceanography, 68(6), 913-927.

Mackey MD, Mackey DJ, Higgins HW (1996) CHEMTAX-a program for estimating class abundances from chemical markers: application to HPLC measurements of phytoplankton. Mar Ecol Prog Ser 144:265–83.

Mantoura, R. F. C., & Wright, S. W. (1997). Phytoplankton pigments in oceanography: guidelines to modern methods. Oceanographic Literature Review, 10(44), 1110.

Matsuno T, J-S Lee, M Shimizu, S-H. Kim, and I-C Pang (2006) Measurements of the turbulent energy dissipation rate ε and an evaluation of the dispersion process of the Changjiang Diluted Water in the East China Sea, J. Geophys. Res., 111, C11S09,

Morimoto A, Takikawa T, Onitsuka G, et al (2009) Seasonal variation of horizontal material transport through the eastern channel of the Tsushima Straits. Journal of oceanography, 65(1), 61-71.

Murphy J, Riley JP (1961) Modified single solution method for the determination of phosphate in natural water. Anal Chem Acta 27:31–36.

Ning X, Lin C, Su J, et al (2011) Long-term changes of dissolved oxygen, hypoxia, and the responses of the ecosystems in the East China Sea from 1975 to 1995. Journal of Oceanography, 67(1), 59-75.

Pan LA, Zhang J, Zhang LH (2007) Picophytoplankton, nanophytoplankton, heterotrohpic bacteria and viruses in the Changjiang Estuary and adjacent coastal waters. J. Plankton Res., 29(2), 187-197.

Partensky F, Hess WR, Vaulot D (1999) Prochlorococcus, a marine photosynthetic prokaryote of global significance. Microbiol. Mol. Biol. Rev. 63:106–127.

Pires, M. D. (2010). Evaluation of Fluorometers for the in situ Monitoring of Chlorophyll and/or Cyanobacteria. Project Report, 1203593-000.

Qian W, Dai M., Xu M, Kao SJ et al (2017) Non-local drivers of the summer hypoxia in the East China Sea off the Changjiang Estuary. Estuarine, Coastal and Shelf Science, 198, 393-399.

Ralf G., & Repeta D. J. (1992). The pigments of Prochlorococcus marinus: The presence of divinylchlorophyll a and b in a marine procaryote. Limnology and Oceanography, 37(2), 425-433.

Redfield AC (1963) The influence of organisms on the composition of seawater. The sea 2:26–77.

Richardson T, Lawrenz E, Pinckney J, Guajardo RC, Waler EA, Paerl HW, MacIntyre HL (2010) Spectral fluorometric characterization of phytoplankton community composition using the Algae Online Analyser. Water Research, 44: 2461–2472.

Roughan ME, Terrill J, Largier JL and Otero MP (2005) Observations of divergence and upwelling around Point Loma, California, J. Geophys. Res., 110, C04011.

Rousseaux CS, Gregg WW (2013) Interannual variation in phytoplankton primary production at a global scale. Remote Sensing 6:1–19.

Salkind NJ (2006) Encyclopedia of measurement and statistics. Sage Publications. pp 566-567.

Sasaki, H., Siswanto, E., Nishiuchi, K., Tanaka, K., Hasegawa, T., & Ishizaka, J. (2008) Mapping the low salinity Changjiang Diluted Water using satellite‐retrieved colored dissolved organic matter (CDOM) in the East China Sea during high river flow season. Geophysical Research Letters, 35, L04604, doi: 10.1029/207GL032637.

See J, Campbell L, Richardson T, Pinckney JL, Shen R, & Guinasso Jr NL (2005) Combining new technologies for determination of phytoplankton community structure in the northern Gul of Mexico, Journal of Phycology, 41: 305–310.

Simpson JH, SharplesJ (2012) Introduction to the physical and biological oceanography of shelf seas. Cambridge University Press. pp 330-343.

Siswanto E, Nakata H, Matsuoka Y (2008) The long-term freshening and nutrient increases in summer surface water in the northern East China Sea in relation to

Changjiang discharge variation. J Geophys Res 113:C10030. doi:10.1029/2008JC004812. Smayda TJ (1997) Harmful algal blooms: their ecophysiology and general relevance to phytoplankton blooms in the sea. Limnology and oceanography.

Sukigara C, Mino Y, Tripathy SC, Ishizaka J, and Matsuno T (2017) Impacts of the Changjiang diluted water on sinking processes of particulate organic matters in the East China Sea. Cont Shelf Res, 151, 84-93.

Suzuki K, Minami C, Liu H and Saino T (2002) Temporal and spatial patterns of chemotaxonomic algal pigments in the subarctic Pacific and Bering Sea during the early summer of 1999. Deep-Sea Res. II, 49, 5685–5704.

Tang X, Wang F, Chen Y, Li M (2009) Warming trend in northern East China Sea in recent four decades. Chin J Oceanol Limnol 27:185–191.

Tseng YF, Lin J, Dai M & Kao SJ (2014) Joint effect of freshwater plume and coastal upwelling on phytoplankton growth off the Changjiang River. Biogeosciences, 11(2), 409.

Uitz J, Stramski D, Reynolds R A, and Dubranna J (2015). Assessing phytoplankton community composition from hyperspectral measurements of phytoplankton absorption coefficient and remote-sensing reflectance in open-ocean environments. Remote Sensing of Environment 171, 58-74.

Umezawa Y, Yamaguchi A, Ishizaka J, et al (2014) Seasonal shifts in the contributions of the Changjiang River and the Kuroshio Current to nitrate dynamics in the continental shelf of the northern East China Sea based on a nitrate dual isotopic composition approach. Biogeosciences, 11, 1297–1317.

Van Heukelem, L., & Thomas, C. S. (2001). Computer-assisted high-performance liquid chromatography method development with applications to the isolation and analysis of phytoplankton pigments. Journal of Chromatography A, 910(1), 31-49.

Wang B, Wang X (2007) Chemical hydrography of coastal upwelling in the East China Sea. Chinese Journal of Oceanology and Limnology, 25(1).

Wang B, Wang X, Zhan R (2003) Nutrient conditions in the Yellow Sea and the East China Sea. Estuarine, Coastal and Shelf Science, 58(1), 127-136.

Wang S, Ishizaka J, Yamaguchi H, et al (2014 a) Influence of the Changjiang River on the light absorption properties of phytoplankton from the East China Sea. Biogeosciences 11:1759–1773.

Wang K, Chen J, Jin H et al. (2014 b) Summer nutrient dynamics and biological carbon uptake rate in the Changjiang River plume inferred using a three end-member mixing model. Cont Shelf Res, 91, 192-200.

Wang K, Chen J, Ni X, Zeng D, et al., (2017) Real-time monitoring of nutrients in the Changjiang Estuary reveals short-term nutrient-algal bloom dynamics. J. Geophys.

Res. Oceans, 122, 5390–5403.

Wang S, Xiao C, Ishizaka J, Qiu Z, Sun D, Xu Q, ... & Watanabe Y (2016) Statistical approach for the retrieval of phytoplankton community structures from in situ fluorescence measurements. Optics Express, 24(21), 23635-23653.

Ward J (1963) Hierarchical Grouping to Optimize an Objective Function. Journal of the American Statistical Association 236–244.

Wong GTF, Gong GC, Liu KK, Pai SC (1998) “Excess Nitrate” in the East China Sea. Estuar Coast Shelf Sci 46:411–418.

Wright S W (2005). Analysis of phytoplankton populations using pigment markers. Course notes for a workshop "Pigment Analysis Of Antarctic Microorganisms”, University of Malaya, June 29 – July 1, 2005.

Wright S, and Jeffrey, S.W. (2006). Pigment Markers for Phytoplankton Production. In Marine Organic Matter: Biomarkers, Isotopes and DNA, J. Volkman, ed. (Springer Berlin Heidelberg), pp. 71-104.

Xu Q, Sukigara C, Goes JI, Gomes HDR, Zhu Y, Wang S, ... & Ishizaka J (2019) Interannual changes in summer phytoplankton community composition in relation to water mass variability in the East China Sea. Journal of Oceanography, 1-19.

Yamaguchi H, Kim HC, Son Y, et al (2012) Seasonal and summer interannual variations of SeaWiFS chlorophyll a in the Yellow Sea and East China Sea. Prog Oceanogr

105:22–29.

Yamaguchi H, Ishizaka J, Siswanto E, et al (2013) Seasonal and spring interannual variations in satellite-observed chlorophyll-a in the Yellow and East China Seas: new datasets with reduced interference from high concentration of resuspended sediment. Cont Shelf Res, 59, 1-9.

Yamamoto, R., Harada, M., Hiramatsu, K., & Tabata, T. (2021). Three-layered Feedforward artificial neural network with dropout for short-term prediction of class-differentiated Chl-a based on weekly water-quality observations in a eutrophic agricultural reservoir. Paddy and Water Environment, 1-18.

Yang D, Yin B, Sun J, Zhang, Y (2013) Numerical study on the origins and the forcing mechanism of the phosphate in upwelling areas off the coast of Zhejiang province, China in summer. Journal of Marine Systems, 123, 1-18.

Yoo S, & Park J (2009) Why is the southwest the most productive region of the East Sea/Sea of Japan?. Journal of Marine Systems, 78(2), 301-315.

Yoshida, M., Horiuchi, T., & Nagasawa Y. (2011) In situ multi-excitation chlorophyll fluorometer for phytoplankton measurements: Technologies and applications beyond conventional fluorometers. OCEANS 2011, 1-4.

Zapata, M., Rodríguez, F., & Garrido, J. L. (2000). Separation of chlorophylls and carotenoids from marine phytoplankton: a new HPLC method using a reversed phase C8 column and pyridine-containing mobile phases. Marine Ecology Progress Series, 195, 29-45.

Zhang J, Liu SM, Ren JL, et al (2007) Nutrient gradients from the eutrophic Changjiang (Yangtze River) Estuary to the oligotrophic Kuroshio waters and re-evaluation of budgets for the East China Sea Shelf. Prog. Oceanogr.

Zhang YY, Dong JD, Ling JA, Wang YS, & Zhang S (2010) Phytoplankton distribution and their relationship to environmental variables in Sanya Bay, South China Sea.

Zhou M, Shen Z, Yu R (2008) Responses of a coastal phytoplankton community to increased nutrient input from the Changjiang (Yangtze) River. Cont Shelf Res 28:1483–1489.

Zhu Y, Ishizaka J, Tripathy SC, et al (2017) Relationship between light, community composition, and the electron requirement for carbon fixation in natural phytoplankton assemblages of the East China Sea. Mar Ecol Prog Ser.

Zhu ZY, Ng WM, Liu SM, et al (2009) Estuarine phytoplankton dynamics and shift of limiting factors: A study in the Changjiang (Yangtze River) Estuary and adjacent area. Estuar Coast Shelf Sci 84:393–401.

Acknowledgements

I would like to thank to my husband Dr. Yao Sun, for who started me up to doctorial course and always be the strong backup force to me. Whenever how many times I said to give up, he would convince me and make me believe I can make it. His unconditionally love supported me throughout the long-time study.

I would like to express my gratitude to all of people who have helped me throughout my doctoral studies in Graduate School of Environmental Studies Nagoya University, Japan .

First of and foremost, my deeply grateful goes to my supervisor Prof. Joji Ishizaka, who is not only the supervisor during my master and doctorial course, but also the wisdom coach of my life. As a supervisor, his rigorous attitude to science impressed me, leading me to think deeply on every scientific questions. As a life coach, he have given me his greatest inclusiveness and supports to me to prove myself and to achieve my goals step by step. Under his guidance, the pleasures that I have obtained from self-actualization exceed the tough of doing research by far.

I am grateful to Prof. Aiki Hidenori, Prof. Yoshihisa Mino, Dr. Chiho Sukigara, and Dr. Akiko Mizuno, they have taught and enhanced my knowledges on different aspect of oceanography. Especial thanks to Dr. Chiho Sukigara, who made great contributions on nutrient measurements.

Particularly grateful to Prof. Joaquim I. Goes and Prof. Helga do Rosario Gomes in Columbia University, they visited our laboratory in 2015. Their genuine opinions straighten out my idea and encouraged me starting to write a paper. When I visited U.S., they spared no effort to support me in every trouble I met, introduced me many famous scientists during the workshop.

Thanks to Dr. Yongjiu Xu, Dr. Shengqiang Wang, Dr. Yuanli Zhu, Dr. Masataka Hayashi and President Takayuki Kusunoki who are like my big brothers, always take care of me whenever in laboratory or during cruise. Special mention goes to Dr. Shengqiang Wang, who gave great contributions on data processing and model development in this study. Thanks to Dr. Elígio Raus Maúre and my dearest Jutarak Luang-on, they almost accompanied with me during the whole master and doctorial course. Thanks to Dr. Chi Feng, Zimeng Li and Yifan Zhang, you are my lovely sisters, brought me joy when I was depressed.

I would also like to thank other members in the Laboratory of Oceanography, Nagoya University, including Takuya Okumura, Takayuki Kusunoki, Koji Tanigawa and Risa Ibuki, Akina Matsushima, Hajime Naganuma, Phattaranakorn Nakornsantiphap for their thought provoking questions, valuable comments and suggestions during each seminar and discussion, which have continuously improved my study. Special thanks also go to laboratory secretariat Mrs. Ayako Watanabe, who always takes care of me like a daughter.

Also Mrs. Ryoko Niizuma, who is willing to help when I was in trouble.

I gratefully acknowledge Ministry of Education, Culture, Sports, Science and Technology (MEXT) for proving me scholarship during my research.

The names mentioned above all contributed to this work. My dream of being a Ph.D will not be achieved without you. Love you all!

Appendices

1. **Inter-annual changes in summer phytoplankton community composition in relation with water mass variability in the East China Sea**

Authors: Qian Xu, Chiho Sukigara, Joaquim I. Goes, Helga do Rosario Gomes, Yuanli Zhu, Shengqiang Wang, Anglu Shen, Elígio de Raús Maúre, Takeshi Matsuno, Watanabe Yuji, Sinjae Yoo, Joji Ishizaka

Published in: *Journal of Oceanography*, 75, pages 61–79 (2019)

2. **High-resolution vertical observations of phytoplankton groups derived from a in situ fluorometer in the East China Sea and Tsushima Strait**

Authors: Qian Xu, Shengqiang Wang, Chiho Sukigara, Joaquim I. Goes, Helga do Rosario Gomes, Takeshi Matsuno, Yuanli Zhu, Yongjiu Xu, Jutarak Luang-on, Yuji Watanabe, Sinjae Yoo, Joji Ishizaka

Accept by: *Frontiers in Marine Science*, Nov., 2021.